Supporting Information

Hyperfluorescent Polymers Enabled by Through-Space Charge Transfer Polystyrene Sensitizers for High-Efficiency and Full-Color Electroluminescence

Jun Hu, Yinuo Wang, Qiang Li, Shiyang Shao,* Lixiang Wang,* Xiabin Jing, and Fosong Wang

This file includes:

- Measurements and characterization details
- Scheme S1-2. Synthetic routes for monomers and polymers
- Figure S1. Comparison of RISC rate constants for TSCT and TBCT polymers.
- Figure S2. PL decay characteristics of fluorescent emitters.
- Figure S3. CV curves and HOMO/LUMO levels for TSCT polystyrenes and corresponding fluorescent emitters.
- Figure S4**.** Optimized geometries and distribution of HONTOs and LUNTOs for hyperfluorescent polymers.
- Figure S5. TGA and DSC characteristics of hyperfluorescent polymers.
- Figure S6. PL spectra of hyperfluorescent polymers and corresponding fluorescent emitter in THF/H_2O mixed solvent.
- Figure S7. Transient PL decay characteristics of hyperfluorescent polymers and TSCT polymer sensitizers in THF/H_2O mixed solvent
- Figure S8. PL decay characteristics of hyperfluorescent polymers.
- Figure S9. PL spectra and decay characteristics of control fluorescent polymers.
- Figure S10. Device performance of blue hyperfluorescent polymers.
- Figure S11. Device performance of green hyperfluorescent polymers.
- Figure S12. Device performance of red hyperfluorescent polymers.
- Figure S13. EL spectra of control fluorescent polymers.
- Figure S14–34. Characterization data for the intermediates and monomers.

Experimental Procedures

General Information. The chemicals and regents were purchased from commercial sources TCI (Shanghai), SigmaAldrich (China) and Energy Chemical (Beijing)) and were used directly. Tetrahydrofuran (THF) and toluene were dried by distillation from sodium/benzophenone, and CH_2Cl_2 was purified by distillation from calcium hydride before use. Mon-Ac, Mon-H, Mon-CF, Mon-CN, BP-H, GP-H and RP-H were synthesized according to procedures in our previous report,[1] PhPe,[2] TBPAD,[3] NTTPA,[4] 4,4,5,5-tetramethyl-2-(perylen-3-yl)-1,3,2-dioxaborolane (**1**),[5] 1,8-bis(4-bromophenyl)octane (**2**),[6] 10-bromo-N,N-bis(4-(tert-butyl)phenyl) anthracen-9-amine (**3**),[7] 4-(9-bromonaphtho[2,3-c][1,2,5]thiadiazol-4-yl)- N,N-diphenylaniline (**7**)[4] and 1-((8-bromooctyl)oxy)-3-vinylbenzene (**9**)[8] were prepared following the procedures in literatures.

Measurements and characterization. ^1H NMR and ^{13}C NMR measurements were carried out on Bruker Avance NMR spectrometer. Elemental analysis was carried out on Bio-Rad elemental analysis system. Matrix-assisted laser desorption/ ionization time of flight (MALDI-TOF) mass spectra were performed on AXIMA CFR MS apparatus (COMPACT). Number/weight-average molecular weight of the polymers were tested by gel permeation chromatography (GPC) on Waters 410 using polystyrene as standard and THF as eluent. Thermal gravimetric analysis (TGA) were measured on Perkin-Elmer-TGA 7, while differential scanning calorimetry (DSC) were performed on PekinElmer-DSC 7 instruments under N_2 at a heating rate of 10 ^oC/min. Cyclic voltammetry curves were recorded on EG&G 283 (Princeton Applied Research) potentiostat/galanostat system, using ferrocene as the reference and n-Bu_4ClO_4 as the supporting electrolyte. The oxidation and reduction curves were recorded in dichloromethane and THF, respectively. The HOMO/LUMO levels were calculated according to the equation E_{HOMO} (or E_{LUMO}) = -e [$E_{onset, ox}$(or $E_{onset, red}$) + 4.8V], where $E_{onset, ox}$ and $E_{onset,red}$ were the onset of the oxidation and reduction waves, respectively. UV-visible absorption spectra were recorded on Perkin-Elmer Lambda 35 UV-vis spectrometer, and photoluminescence spectra were measured on FluoroMax spectrofluorometer. The PLQYs were measured by integrating sphere on Hamamatsu Photonics C9920-2. PL decay curves were recorded using Edinburgh fluorescence spectrometer (FLSP-980).

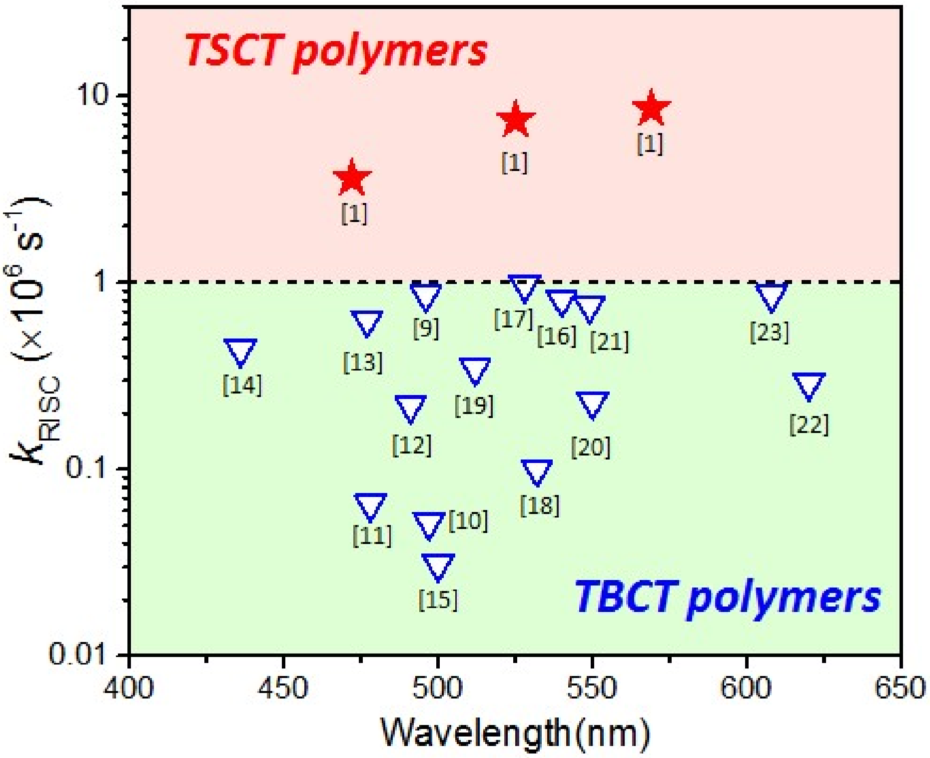

Figure S1. Comparison of RISC rate constant (k_{RISC}) values between through-space charge transfer (TSCT) TADF polymers used in this work and through-bond charge transfer (TBCT) TADF polymers in literatures.

Table S1. k_{RISC} values for TBCT polymers in literatures.

Polymer	**Chemical Structure**	**Emission Peak (nm)**	**k_{RISC} (10^6 s^{-1})**	**CIE (x, y)**	**Ref.**
PCzDP-10	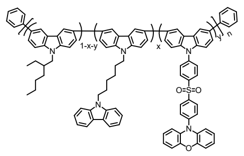	496	**0.86**	0.22, 0.40	[9]
P3	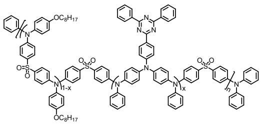	497	**0.052**	0.22, 0.35	[10]
PBD-10	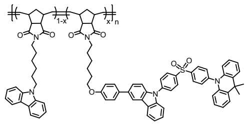	478	**0.065**	0.20, 0.29	[11]

PACDPS-12	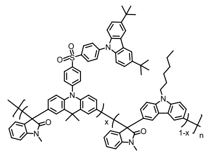	491	**0.22**	0.22, 0.39	[12]
P(BOPACTRZ-BPA)	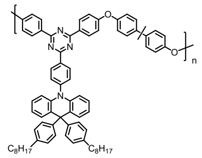	477	**0.63**	0.18, 0.32	[13]
PDT-2	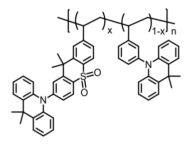	436	**0.44**	0.15, 0.09	[14]
pCzBP	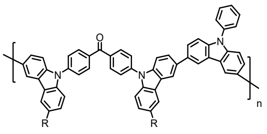	500	**0.031**	0.28, 0.43	[15]
POPT-25	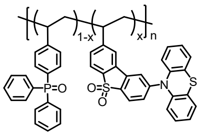	540	**0.81**	0.36, 0.50	[16]
P(DMTRZ-Cp)	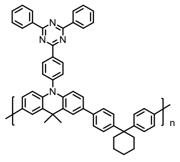	528	**1.07**	0.35, 0.57	[17]
poly(TPAm-DCBm)	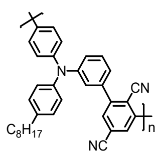	532	**0.10**	0.34, 0.57	[18]
poly(TMTPA-DCB)	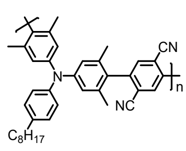	512	**0.35**	0.34, 0.57	[19]
P9	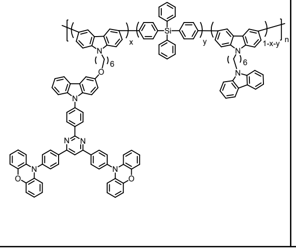	550	**0.23**	0.41,0.54	[20]

PCzBPCl-10	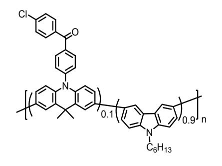	549	**0.75**	0.39,0.56	[21]
PCzAQC0.5	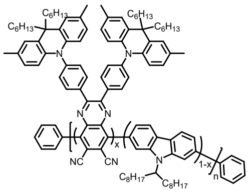	620	**0.29**	0.56, 0.42	[22]
PSAQF10	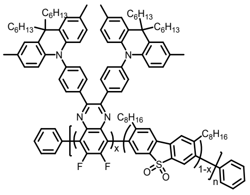	608	**0.86**	0.48, 49	[23]

Table S2. k_{RISC} values for TSCT polymers used in this work.

Polymer	**Chemical Structure**	**Emission Peak (nm)**	**k_{RISC} (10^6 s^{-1})**	**CIE (x, y)**	**Ref.**
BP-H	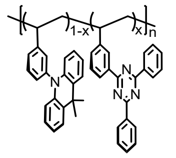	472	**3.6**	0.18, 0.27	[1]
GP-H	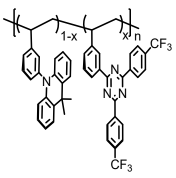	525	**7.4**	0.34, 0.55	[1]
RP-H	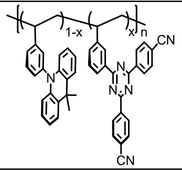	569	**8.5**	0.46, 0.50	[1]

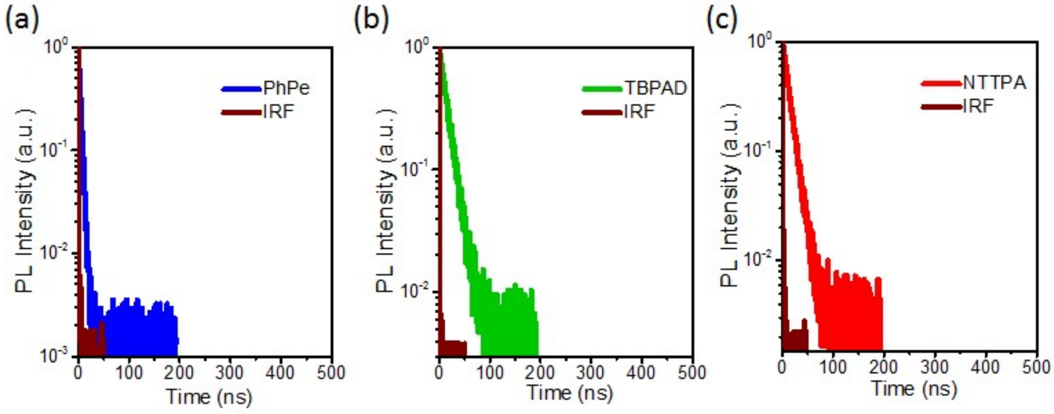

Figure S2. PL decay curves of fluorescent emitters in toluene (1×10^{-5} mol L^{-1})

Table S3. Summary of photophysical properties of fluorescent emitters.

	λ_{abs} [a] (nm)	λ_{em} [b] (nm)	τ [c] (ns)	PLQY [d] (%)	S_1 [e] (eV)
PhPe	418/447	463	4.0	94	2.79
TBPAD	361/471	528	14.4	90	2.51
NTTPA	350/511	646	12.4	75	2.18

[a] Absorption peak measured in dichloromethane (1×10^{-5} mol L^{-1}); [b] emission peak measured in toluene (1×10^{-5} mol L^{-1}); [c] lifetime of fluorescence; [d] absolute PL quantum yield measured in toluene (1×10^{-5} mol L^{-1}) by integrating sphere; [e] singlet energy obtained from onset of fluorescence.

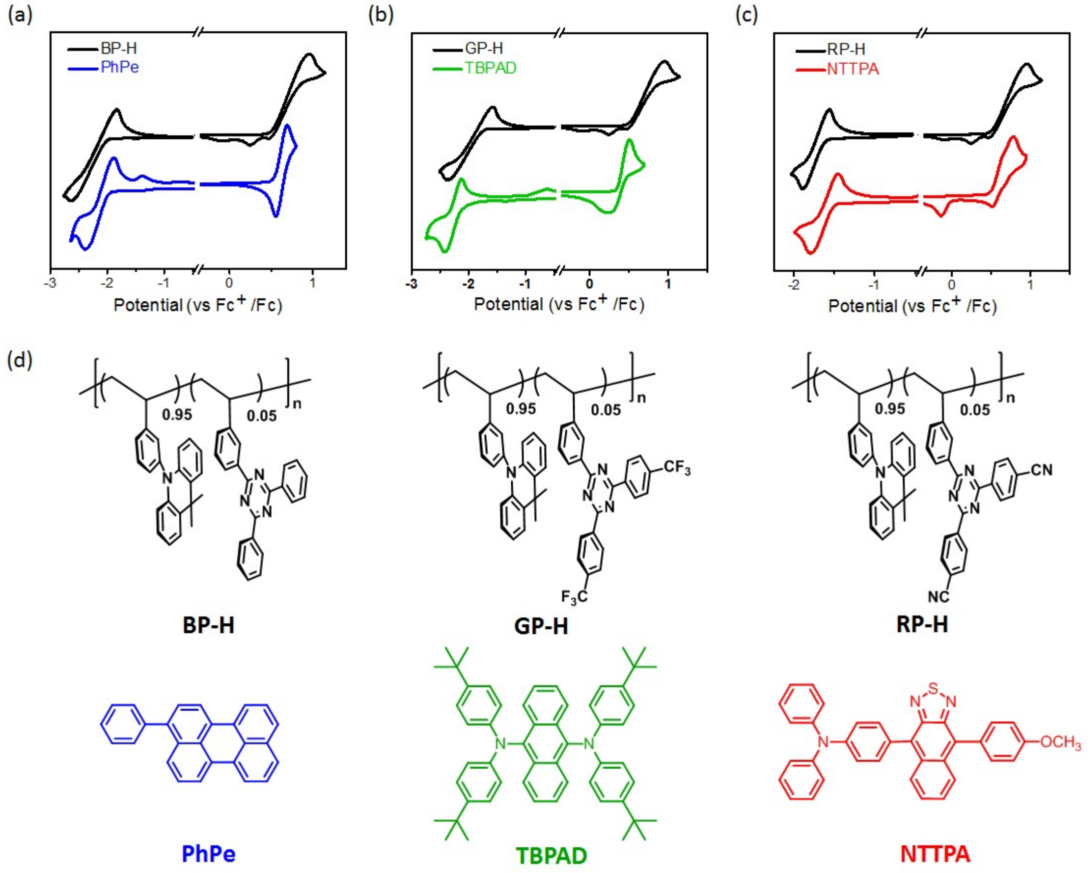

Figure S3. Cyclic voltammetry (CV) characteristics for TSCT polymers and corresponding fluorescent emitters.

Table S4. Summary of CV properties of TSCT polymers and fluorescent emitters.

		$E_{onset,ox}$ [a] (V)	$E_{onset, red}$ [b] (V)	E_{HOMO} [c] (eV)	E_{LUMO} [d] (eV)
Blue	BP-H	0.48	-2.12	-5.28	-2.68
	PhPe	0.52	-1.99	-5.32	-2.81
Green	GP-H	0.48	-1.80	-5.28	-3.00
	TBPAD	0.35	-1.97	-5.15	-2.83
Red	RP-H	0.48	-1.66	-5.28	-3.14
	NTTPA	0.50	-1.51	-5.30	-3.29

[a] Onset of oxidation potential; [b] Onset of reduction potential; [c] HOMO energy level; [d] LUMO energy level.

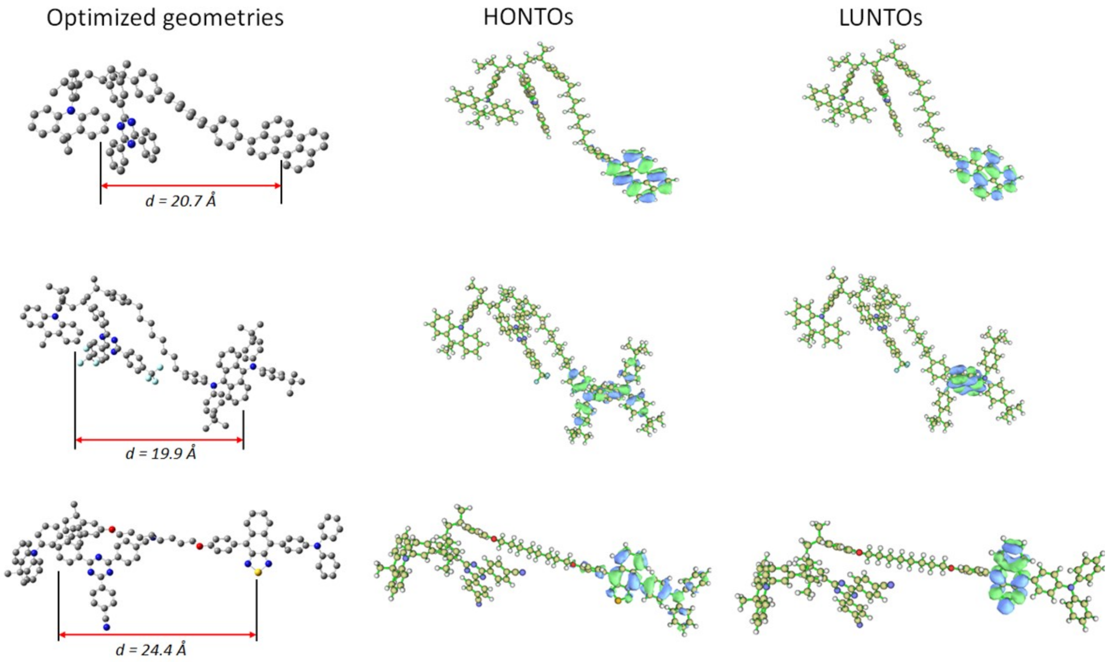

Figure S4. Optimized geometries and distribution of HONTOs and LUNTOs for hyperfluorescent polymers (top: blue polymer, middle: green polymer, bottom: red polymer) using a donor, an acceptor and an emitter as model (geometry optimized at B3LYP/6-31G(d) level and HONTOs/LUNTOs simulated at (PBE0-1/3)/6-31G(d) level).

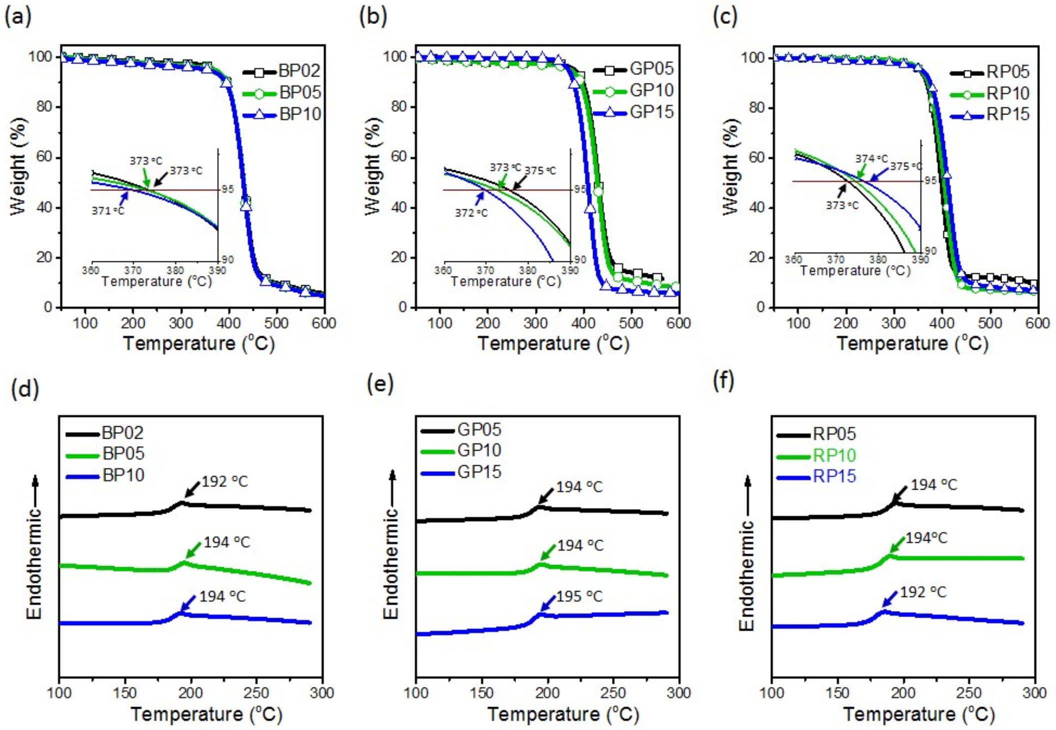

Figure S5. Thermogravimetic analysis (TGA) and differential scanning calorimetry (DSC) characteristics for hyperfluorescent polymers.

Table S5. Summary of decomposition temperatures (T_d) and glass transition temperatures (T_g) for hyperfluorescent polymers.

	Blue			Green			Red		
	BP02	BP05	BP10	GP05	GP10	GP15	RP05	RP10	RP15
T_d (°C) [a]	373	373	371	375	373	372	373	374	375
T_g (°C)	192	194	194	194	194	195	194	194	192

[a] Corresponding to 5% weight loss.

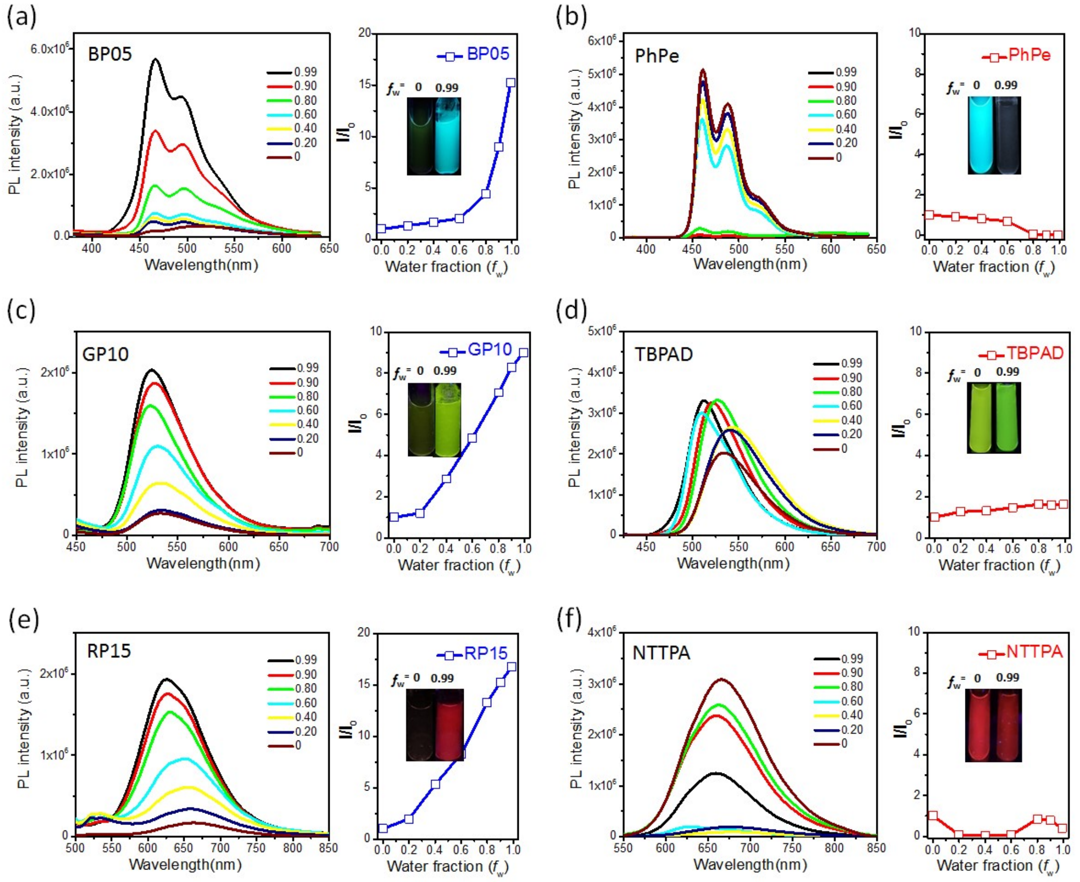

Figure S6. PL spectra and relative emission intensity of hyperfluorescent polymers and fluorescent emitters in THF/H_2O mixed solvents (concentration of 1×10^{-5} M) with different water fractions (f_w).

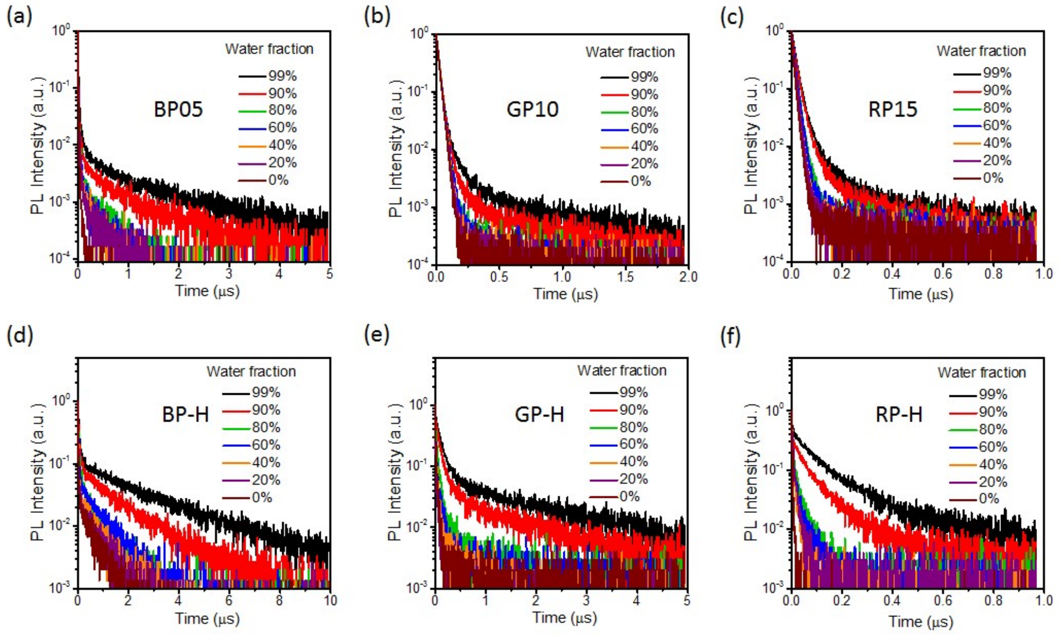

Figure S7. Transient PL decay characteristics for hyperfluorescent polymers and TSCT polymer sensitizers in THF/H_2O mixture.

Table S6. Summary of lifetimes for TSCT polymer sensitizers and hyperfluorescent polymers in THF/H_2O mixtures.

Water fraction	τ_p[a]/τ_d[b] (ns/μs)					
	BP-H	BP05	GP-H	GP10	RP-H	RP15
99%	30.8/1.70	12.5/0.68	38.6/1.1	18.3/0.51	39.2/0.75	19.6/0.23
90%	25.3/1.30	10.3/0.39	32.5/0.93	16.4/0.37	26.4/0.56	17.4/0.19
80%	20.5/0.83	9.6/0.26	27.4/0.57	10.3/0.18	11.8/0.16	8.3/--
60%	17.7/0.62	8.90/0.19	18.7/0.48	9.8/0.15	10.3/0.13	7.9/--
40%	15.8/0.60	8.7/0.18	16.3/0.41	8.8/0.14	9.5/--	7.3/--
20%	14.1/0.53	8.5/0.16	15.7/0.25	8.4/--	9.1/--	6.7/--
0	11.2/0.47	5.1/--[c]	12.3/0.21	4.8/--	8.7/--	4.7/--

[a] Lifetime of prompt fluorescence; [b] Lifetime of delayed fluorescence; [c] Delayed fluorescence is too weak to be detected in these conditions.

Table S7. Summary of photophysical properties of hyperfluorescent polymers.

	Polymer	τ_p [a] (ns)	τ_d [b] (µs)	$1/\tau_p$ (10^7 s^{-1})	k_{FRET} [c] (10^7 s^{-1})
Blue	BP-H	36.0	1.28	2.8	/
	BP02	12.1	0.76	8.3	5.5
	BP05	11.2	0.75	9.1	6.3
	BP10	10.1	0.66	10.0	7.2
Green	GP-H	40.0	1.20	2.5	/
	GP05	17.4	0.99	5.9	3.4
	GP10	16.6	0.93	6.3	3.8
	GP15	14.5	0.86	7.1	4.6
Red	RP-H	47.0	1.14	2.1	/
	RP05	24.4	0.90	4.2	2.1
	RP10	20.8	0.85	4.8	2.7
	RP15	18.0	0.79	5.5	3.4

[a] Lifetime of prompt fluorescence; [b] Lifetime of delayed fluorescence; [c] Rate constant for FRET process.

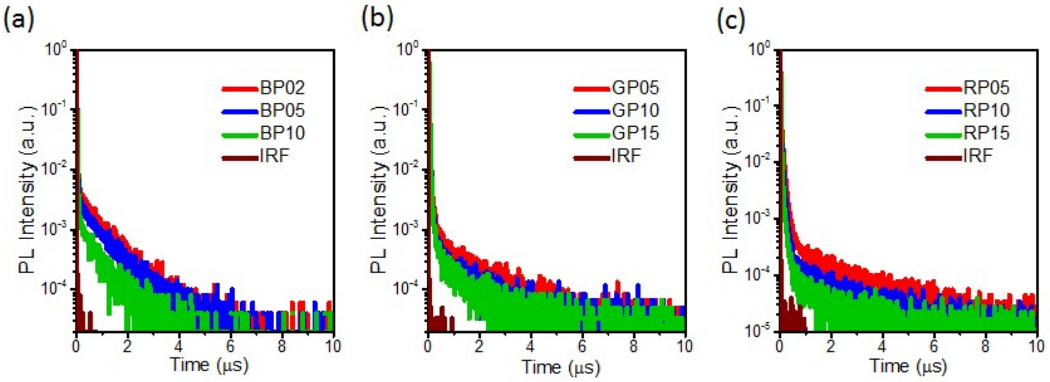

Figure S8. PL decay curves for BP02~BP10 monitored at 466 nm (a), GP05~GP15 monitored at 530 nm (b), and RP05~RP15 monitored at 640 nm (c).

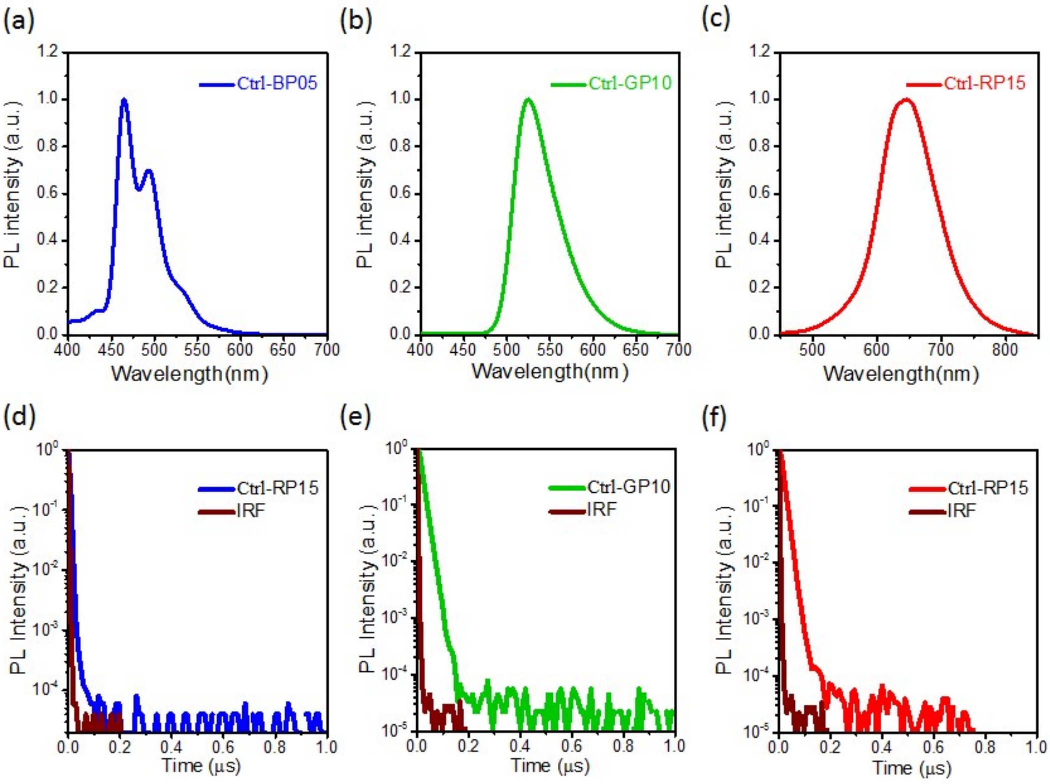

Figure S9. PL spectra (a-c) and PL decay curves (d-f) of control fluorescent polymers in toluene solution (1×10^{-5} mol L^{-1}).

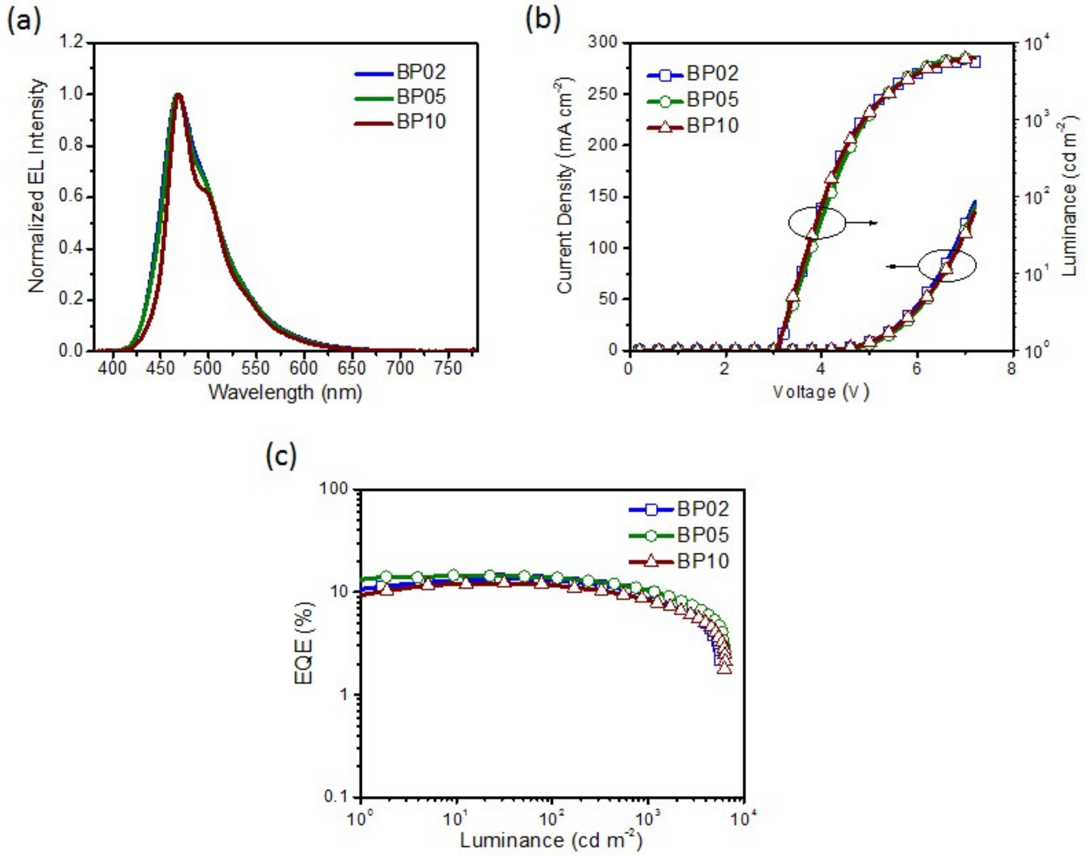

Figure S10. EL spectra (a), current density (*J*) – voltage (*V*) – luminance (*L*) (b) and EQE–*L* characteristics (c) of solution-processed OLEDs based on BP02, BP05 and BP10.

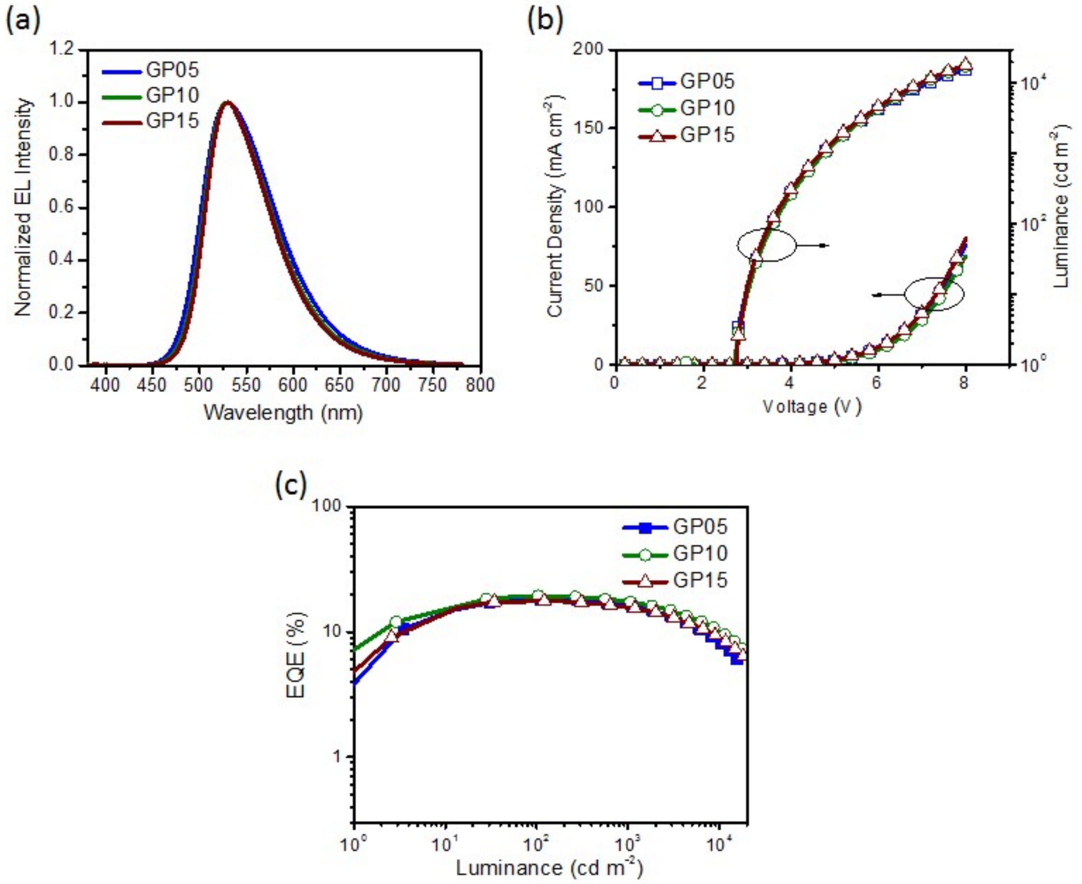

Figure S11. EL spectra (a), *J*–*V*–*L* (b) and EQE–*L* characteristics (c) of solution-processed OLEDs based on GP05, GP10 and GP15.

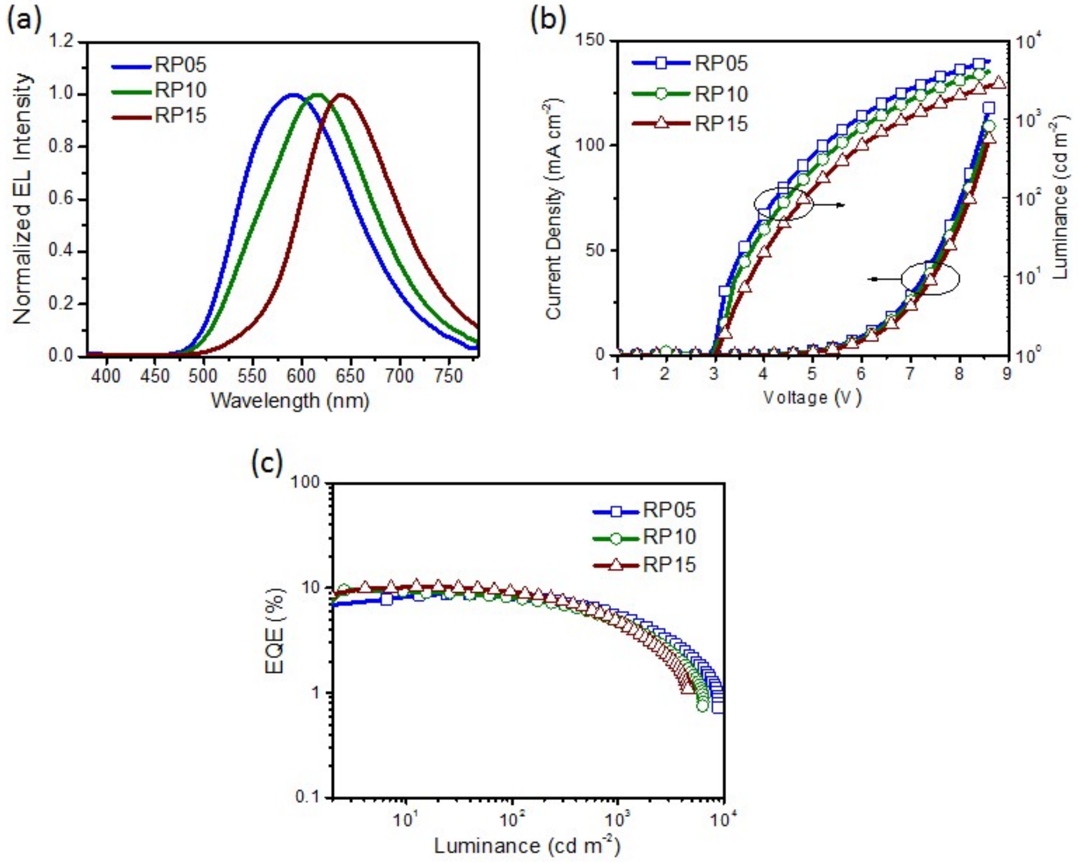

Figure S12. EL spectra (a), *J*–*V*–*L* (b) and EQE–*L* characteristics (c) of solution-processed OLEDs based on RP05, RP10 and RP15.

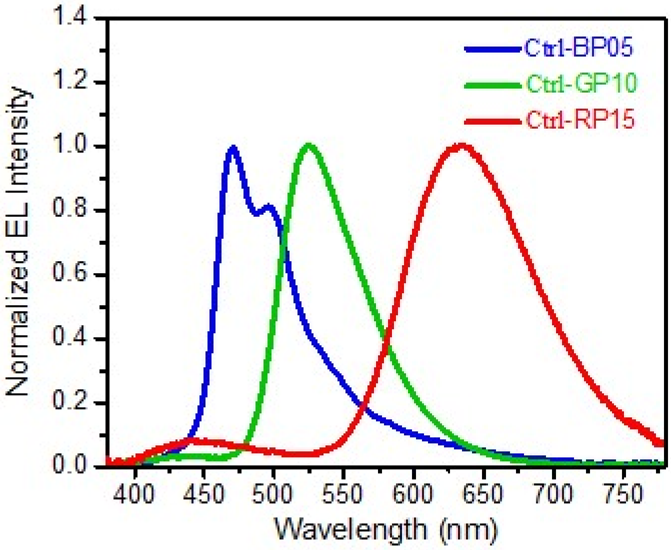

Figure S13. EL spectra for solution-processed OLEDs based on Ctrl-BP05, Ctrl-GP10 and Ctrl-RP15.

Table S8. Calculation of exciton utilization ratio for solution-processed OLEDs.

	Polymer	PLQY[a] (%)	EQE[b] (%)	η_{ST}[c] (%)
Blue	BP02	81	13.5	66.7
	BP05	83	14.6	70.4
	BP10	82	12.2	59.5
	Ctrl-BP05	82	3.0	14.6
Green	GP05	81	18.2	89.9
	GP10	82	19.2	93.7
	GP15	82	17.6	85.9
	Ctrl-GP10	83	3.6	17.3
Red	RP05	65	8.8	54.2
	RP10	65	9.6	59.1
	RP15	64	10.3	64.4
	Ctrl-RP15	62	2.0	12.9

[a] Photoluminescence quantum efficiency measured in solid-state film; [b] Maximum external quantum efficiency for solution-processed OLEDs; [c] exciton utilization ratio for the devices assuming light out-coupling efficiency of 0.25.

Scheme S1. Synthetic routes for emitter-containing monomers.

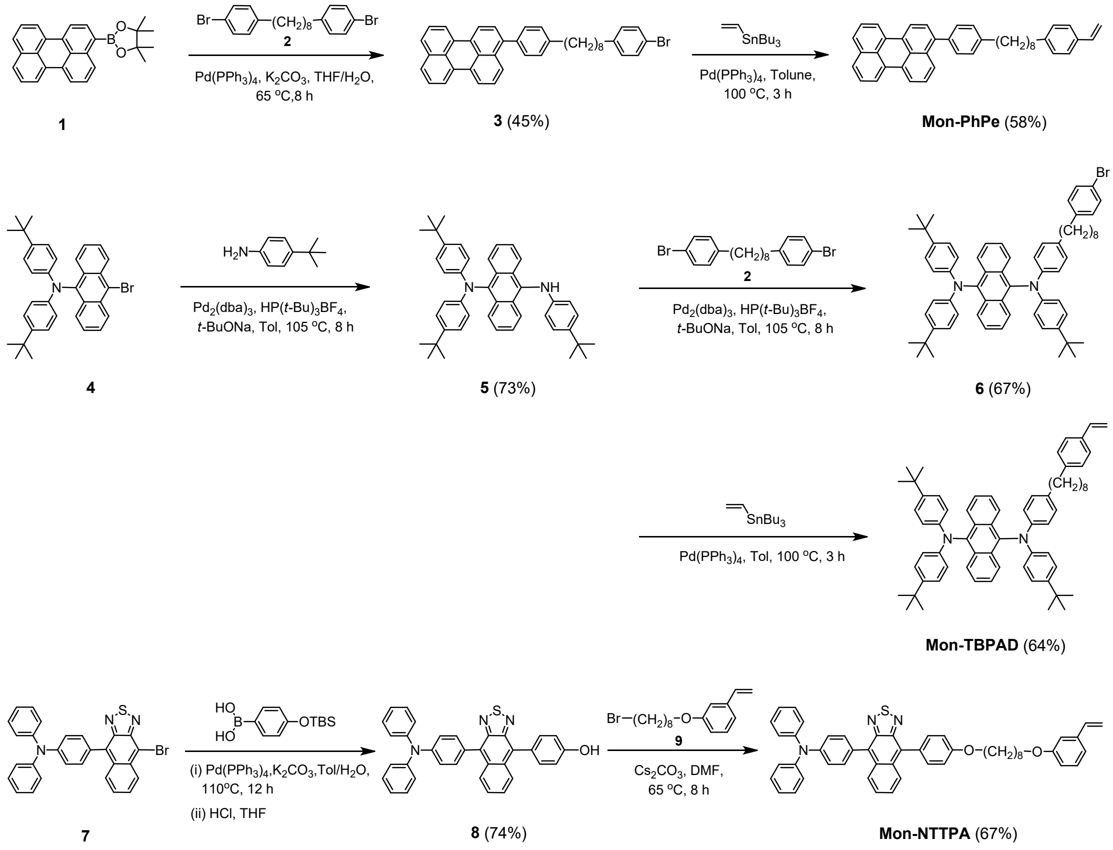

Scheme S2. Synthetic routes for hyperfluorescent polymers.

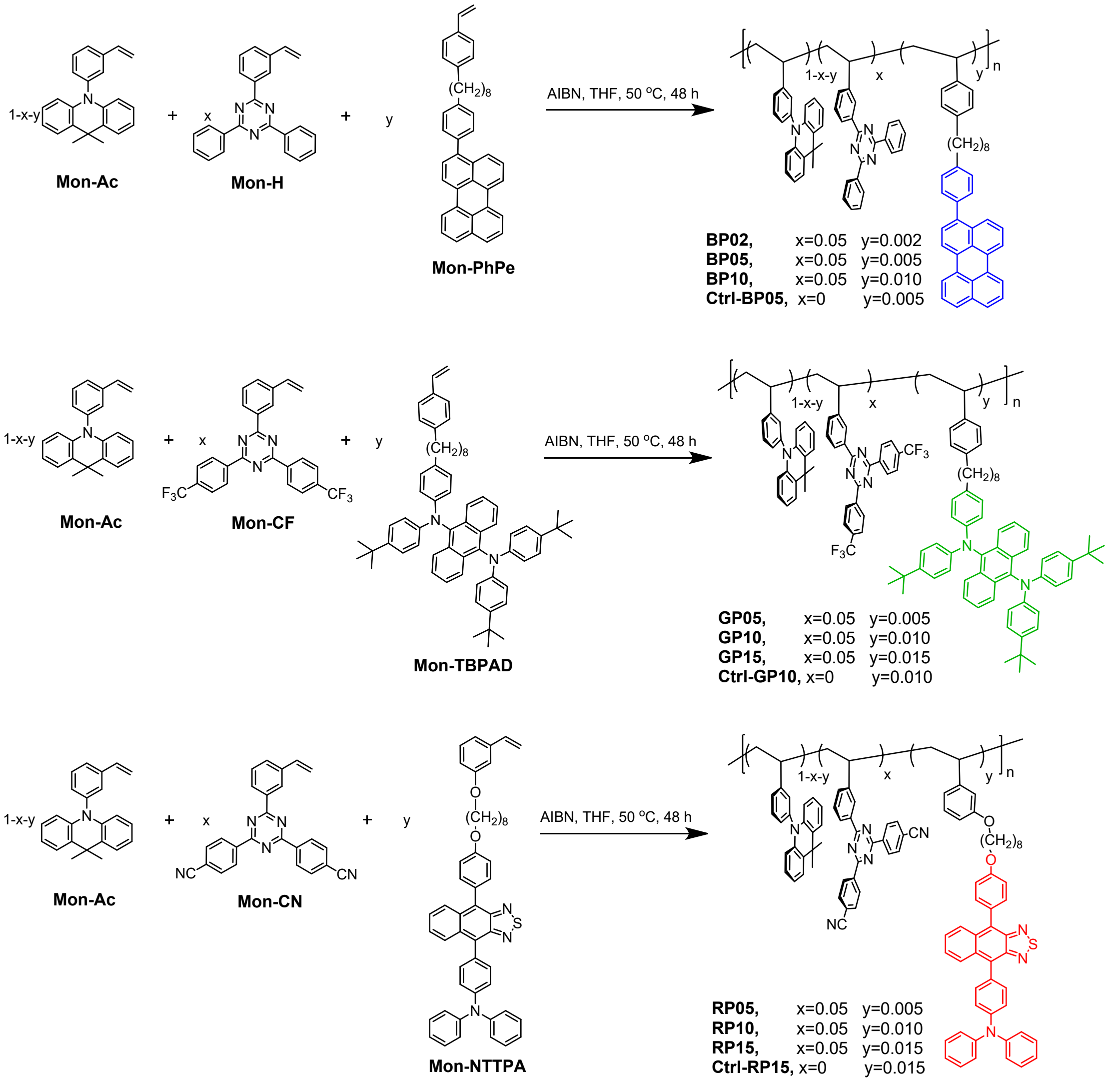

*3-(4-(8-(4-bromophenyl)octyl)phenyl)perylene (**3**)*

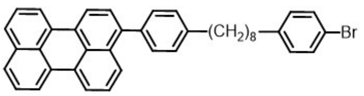

A mixture of 4,4,5,5-tetramethyl-2-(perylen-3-yl)-1,3,2-dioxaborolane (**1**) (1.13 g, 3.0 mmol), 1,8-bis(4-bromophenyl)octane (**2**) (1.91 g, 4.5 mmol) , $Pd(PPh_3)_4$ (0.17 g, 0.15 mmol) and K_2CO_3 (1.24 g , 9.0 mmol) in 80 ml THF and 20 ml water was stirred at 65 ^oC under argon atmosphere for 8 hours. After cooling to room temperature, the mixture was diluted with CH_2Cl_2 (100 mL) and washed with brine three times (100 mL×3). Then the organic phase was dried with anhydrous sodium sulfate and the solvent was removed under vacuum. The residue was applied to silica gel colume using cyclohexane as eluent to afford the product as a yellow solid in a yeild of 45%. ^1H NMR (500 MHz, $CDCl_3$) δ 8.25 – 8.19 (m, 4H), 7.80 (d, *J* = 8.4 Hz, 1H), 7.69 (d, *J* = 8.1 Hz, 2H), 7.52 – 7.47 (m, 2H), 7.43 (m, 3H), 7.41 – 7.37 (m, 2H), 7.31 (d, *J* = 8.0 Hz, 2H), 7.05 (d, *J* = 8.3 Hz, 2H), 2.71 (t, *J* =7.7 Hz, 2H), 2.50 t, *J* =7.7 Hz, 2H), 1.73–1.67 (m, 2H), 1.64 – 1.56 (m, 2H), 1.42 – 1.31 (m, 8H). ^{13}C NMR (126 MHz, $CDCl_3$) δ 142.09, 141.81, 140.04, 137.99, 134.71, 133.02, 131.47, 131.37, 131.32, 131.25, 130.42, 130.17, 129.82, 129.09, 128.67, 128.39, 127.71, 126.60, 126.39, 126.22, 120.32, 120.28, 120.03, 119.97, 119.25, 35.76, 35.35, 31.50, 31.32, 29.45, 29.41, 29.18. MALDI-TOF: calcd for $C_{40}H_{35}Br$: 594.2, found: 594.2 [M^+], Anal: Calcd for $C_{40}H_{35}Br$: C, 80.66; H, 5.92; found: C, 80.53; H, 5.82.

*3-(4-(8-(4-vinylphenyl)octyl)phenyl)perylene (**Mon-PhPe**)*

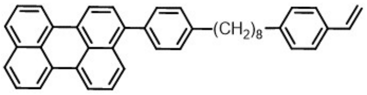

A mixture of 3-(4-(8-(4-bromophenyl)octyl)phenyl) perylene (**3**) (0.60 g, 1.0 mmol), tributyl(vinyl)stannane (0.47 g, 1.5 mmol), and $Pd(PPh_3)_4$ (0.06 g, 0.05 mmol) in 20 ml toluene was stirred at 100 ^oC under argon atmosphere for 3 hours. After cooling to room temperature, the reaction was quenched by 20 mL satureted potassium fluoride aqueous solution. The organic phase was washed with brine three times (40 mL×3) and then dried with anhydrous sodium sulfate. After removing the solvent under vacuum, the residue was applied to silica gel colume using cyclohexane as eluent to afford the product as a yellow solid in yeild of 58%. ^{1}H NMR (500 MHz, $CDCl_3$) δ 8.26 – 8.18 (m, 4H), 7.80 (d, *J* = 8.4Hz, 1H), 7.69 (d, *J* = 8.1 Hz, 2H), 7.51 – 7.46 (m, 2H), 7.42 (t, *J* = 8.2 Hz, 4H), 7.32 (t, *J* = 8.6 Hz, 4H), 7.14 (d, *J* = 8.0 Hz, 2H), 6.69 (dd, *J* = 17.6, 10.9 Hz, 1H), 5.70 (d, *J* = 17.6, 1H), 5.18 (d, *J* = 10.9 Hz, 1H), 2.70 (t, *J* = 7.7 Hz, 2H), 2.60 (t, *J* = 7.7 Hz, 2H), 1.74 – 1.66 (m, 2H), 1.66 – 1.58 (m, 2H), 1.43 – 1.32 (m, 8H). ^{13}C NMR (126 MHz, $CDCl_3$) δ 142.70, 142.12, 140.06, 137.98, 136.73, 135.04, 134.71, 133.03, 131.49, 131.37, 131.33, 130.41, 129.82, 129.09, 128.68, 128.57, 128.40, 127.72, 127.66, 126.61, 126.60, 126.39, 126.24, 126.12, 120.31, 120.27, 120.02, 119.97, 112.80, 35.77, 35.70, 31.51, 31.44, 29.47, 29.42, 29.30. MALDI-TOF: calcd for $C_{42}H_{38}$: 542.3, found: 542.3 [M$^+$], Anal: Calcd for $C_{42}H_{38}$: C, 92.94; H, 7.06; found: C, 92.93; H, 6.98.

*N^9,N^9,N^{10}-tris(4-(tert-butyl)phenyl)anthracene-9,10-diamine (**5**)*

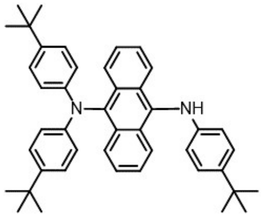

A mixture of 10-bromo-*N,N*-bis(4-(tert-butyl)phenyl) anthracen-9-amine (**4**) (3.21 g, 6.0 mmol), 4-(*tert*-butyl)aniline (1.35 g, 9.0 mmol), $Pd_2(dba)_3$ (0.27 g, 0.3 mmol), $(t\text{-}Bu)_3HP\text{-}BF_4$ (0.35 g, 1.2 mmol) and *t*-BuONa (1.15 g, 12.0 mmol) in toluene (50 mL) was stirred at 105 °C under argon for 8 hours. After cooling to room temperature, 200 mL CH_2Cl_2 was added to dilute the solution. The organic phase was washed with brine three times (200 mL×3) and then dried with anhydrous sodium sulfate. After the solvent was removed under vaccum, the residue was applied to a silica gel colume using cyclohexane/dichloromethane = 25/1 (v/v) as eluent to afford the product as a yellow solid in yelid of 73%. ^{1}H NMR (400 MHz, DMSO) δ 8.39 (s, 1H), 8.28 – 8.22 (m, 2H), 8.09 – 8.03 (m, 2H), 7.24 – 7.18 (m, 4H), 7.11 (d, *J* = 8.8 Hz, 2H), 6.93 – 6.88 (m, 4H), 6.49 (d, *J* = 8.7 Hz, 2H), 1.21 (s, 27H). ^{13}C NMR (126 MHz, $CDCl_3$) δ 145.50, 145.26, 143.42, 141.49, 136.08, 133.06, 131.45, 130.06, 126.55, 126.10, 125.86, 125.22, 124.50, 119.48, 113.78, 34.07, 33.95, 31.52, 31.40, 26.91, 22.66, 14.13. MALDI-TOF: calcd for $C_{44}H_{48}N_2$: 604.4, found: 604.4 [M$^+$], Anal: Calcd for $C_{44}H_{48}N_2$: C, 87.37; H, 8.00, N, 4.63; found: C, 87.28; H, 7.87, N, 4.72.

*N^9-(4-(8-(4-bromophenyl)octyl)phenyl)-N^9,N^{10},N^{10}-tris(4-(tertbutyl)phenyl)anthracene-9,10-diamine (**6**)*

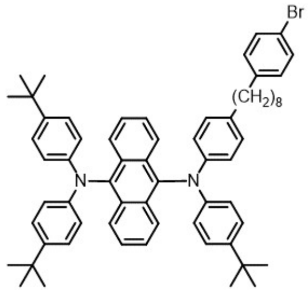

A mixture of N^9,N^9,N^{10}-tris(4-(tert-butyl)phenyl)anthracene-9,10-diamine (**5**) (2.67 g, 4.0 mmol), 1,8-bis(4-bromophenyl)octane (**2**) (2.54 g, 6.0 mmol), $Pd_2(dba)_3$ (0.18 g, 0.2 mmol), (*t*-Bu)$_3$HP-BF$_4$ (0.23 g, 0.8 mmol) and *t*-BuONa (1.15 g, 12.0 mmol) in toluene (50 mL) was stirred at 105 °C under argon for 8 hours. After cooling to room temperature, the solution was diluted with 200 mL CH_2Cl_2. The organic phase was washed with brine three times (200 mL×3) and then dried with anhydrous sodium sulfate. After the solvent was removed under vacuum, the residue was applied to silica gel colume using cyclohexane as eluent to afford the product as a yellow solid in yeild of 67%. ^{1}H NMR (500 MHz, $CDCl_3$) δ 8.18 (s, 4H), 7.37 (d, *J* = 8.3 Hz, 2H), 7.33 (dd, *J* = 6.7, 2.8 Hz, 4H), 7.18 (d, *J* = 8.2 Hz, 6H), 7.00 (dd, *J* = 28.4, 8.0 Hz, 12H), 2.60 – 2.44 (m, 4H), 1.60 – 1.50 (m, 4H), 1.28 (s, 8H), 1.26 (s, 27H). ^{13}C NMR (126 MHz, $CDCl_3$) δ 145.65, 145.27, 143.53, 141.81, 137.50, 132.03, 131.96, 131.24, 130.16, 129.00, 128.59, 128.39, 128.20, 126.50, 125.95, 125.34, 125.27, 119.98, 119.57, 119.23, 35.33, 35.21, 34.09, 31.41, 31.30, 29.71, 29.40, 29.36, 29.15, 26.92, 14.12. MALDI-TOF: calcd for $C_{64}H_{71}BrN_2$: 946.5, found: 946.5 [M$^+$], Anal: Calcd for $C_{64}H_{71}BrN_2$: C, 81.07; H, 7.55, N, 2.95; found: C, 81.18; H, 7.46, N, 2.87.

*N^9,N^9,N^{10}-tris(4-(tert-butyl)phenyl)-N^{10}-(4-(8-(4-vinylphenyl)octyl)phenyl)anthracene-9,10-diamine (**Mon-TBPAD**)*

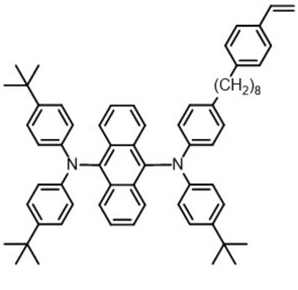

A mixture of N^9-(4-(8-(4-bromophenyl)octyl)phenyl)-N^9,N^{10},N^{10}-tris(4-(tertbutyl)phenyl)anthracene-9,10-diamine (**6**) (1.90 g, 2.0 mmol), tributyl(vinyl)stannane (0.95 g, 3.0 mmol) and $Pd(PPh_3)_4$ (0.12 g, 0.1 mmol) in toluene (30 mL) was stirred at 105 °C under argon for 3 hours. After cooling to room temperature, the reaction was quenched with 30 mL satureted potassium fluoride aqueous solution. The organic phase was washed with brine three times (40 mL×3), and then dried with anhydrous sodium sulfate. After the solvent was removed under vacuum, the residue was applied to silica gel colume using cycolhexane as eluent to afford the product as a yellow solid in yeild of 64%. ^{1}H NMR (500 MHz, $CDCl_3$) δ 8.18 (d, *J* = 6.3 Hz, 4H), 7.36 – 7.29 (m, 6H), 7.17 (t, *J* = 7.6 Hz, 6H), 7.13 (t, *J* = 6.7 Hz, 2H), 7.07 – 6.94 (m, 10H), 6.68 (dd, *J* = 17.6, 10.9 Hz, 1H), 5.69 (d, *J* = 17.6 Hz, 1H), 5.17 (d, *J* = 10.9 Hz, 1H), 2.58 (t, *J* = 7.8 Hz, 2H), 2.49 (s, 2H), 1.61 – 1.52 (m, 4H), 1.30 (s, 8H), 1.26 (s, 27H). ^{13}C NMR (126 MHz, $CDCl_3$) δ 145.25, 143.55, 142.71, 137.48, 136.73, 135.02, 132.03, 129.01, 128.56, 128.39, 128.20, 126.50, 126.10, 125.94, 125.53, 125.34, 125.28, 119.99, 119.58, 112.77, 35.97, 35.67, 35.21, 34.09, 31.42, 29.71, 29.43, 29.37, 29.31, 29.27. MALDI-TOF: calcd for $C_{66}H_{71}N_2$: 894.6, found: 894.6 [M$^+$], Anal: Calcd for $C_{66}H_{71}N_2$: C,88.54; H,8.33; N, 3.13; found: C, 88.43; H, 8.20; N, 3.05.

*4-(9-(4-(diphenylamino)phenyl)naphtho[2,3-c][1,2,5]thiadiazol-4-yl)phenol (**8**)*

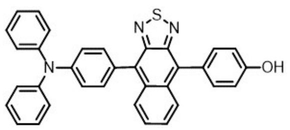

A mixture of 4-(9-bromonaphtho[2,3-c][1,2,5]thiadiazol -4-yl)-*N,N*-diphenylaniline (**7**) (0.61 g, 1.2 mmol), (4-((*tert*-butyldimethylsilyl)oxy)phenyl)boronic acid (0.40 g, 1.56 mmol), $Pd(PPh_3)_4$ (0.07 g, 0.06 mmol), toluene (20 mL) and K_2CO_3 aqueous solution (2 M, 4 mL) was stirred at 110 ^{o}C under argon for 12 hours. After cooling to room temperature, the organic phase was separated and dried over anhydrous sodium sulfate. The solvent was removed under vacuum, and the residue was applied to silica gel using hexane/dichloromethane = 8/1 (v/v) as eluent to afford the intermediate with protecting group as a red solid in yeild of 74%. ^{1}H NMR (500 MHz, DMSO-*d*$_6$) δ 8.04 (d, *J* = 7.9 Hz, 1H), 7.93 (d, *J* = 7.8 Hz, 1H), 7.55 (dd, *J* = 13.2, 8.5 Hz, 4H), 7.51 – 7.44 (m, 2H), 7.40 (t, *J* = 7.8 Hz, 4H), 7.19 (t, *J* = 7.4 Hz, 6H), 7.12 (dd, *J* = 16.9, 7.9 Hz, 4H), 1.03 (s, 9H), 0.31 (s, 6H). ^{13}C NMR (126 MHz, $CDCl_3$) δ 155.77, 151.64, 151.47, 147.73, 147.56, 132.48, 132.18, 132.04, 129.74, 129.41, 129.25, 127.19, 126.13, 125.14, 123.39, 122.23, 119.91, 25.71, 18.24. MALDI-TOF: calcd for

$C_{40}H_{37}N_3OSSi$: 635.2, found: 635.2 [M^+], Anal: Calcd for $C_{40}H_{37}N_3OSSi$: C, 75.55; H, 5.87, N, 6.61, S, 5.04; found: C, 75.64; H, 5.93, N, 6.53, S, 4.98.

A mixture of the protected intermediate (0.32 g, 0.5 mmol), 30 mL THF and HCl aqueous solution (2 M, 15 mL) was stirred at room temperature for 48 h. Then the mixture was extracted with CH_2Cl_2 three times (30 mL×3), and the combined organic phase was washed with brine (50 mL×3). After drying the organic phase by anhrdrous sodium sulfate, the solvent was removed under vacuum to afford the product as a red solid, which was used directly for next step.

*N,N-diphenyl-4-(9-(4-((8-(3-vinylphenoxy)octyl)oxy)phenyl)naphtho[2,3-c][1,2,5] thiadiazol-4-yl)aniline (**Mon-NTTPA**)*

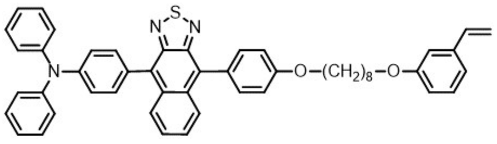

A mixture of phenol4-(9-(4-(diphenylamino)phenyl)naphtho[2,3-c][1,2,5]thiadiazol-4-yl)phenol (**8**) (0.15 g, 0.3 mmol), 1-((8-bromooctyl)oxy)-3-vinylbenzene (**9**) (0.16 g, 0.5 mmol) and Cs_2CO_3 (0.20 g, 0.6 mmol) were added to 30 mL DMF and stirred at 65 ^oC under argon for 8 hours. After cooling to room temperature, the mixture was poured into water (100 mL) and extracted with $CHCl_3$ (50 mL×3). The combined organic phase was washed with brine (200 mL×3) and dried over anhydrous sodium sulfate. After the solvent was removed under vacuum, the residue was applied to silica gel colum using hexane/dochloromethane = 8/1 (v/v) as eluent to give the product as a red solid in yeild of 67%. ^1H NMR (500 MHz, C_6D_6) δ 8.34 – 8.30 (m, 1H), 8.26 – 8.21 (m, 1H), 7.67 – 7.63 (m, 2H), 7.63 – 7.57 (m, 2H), 7.34 – 7.29 (m, 2H), 7.20 (dd, *J* = 9.3, 5.7, 3.6 Hz, 4H), 7.13 – 7.04 (m, 10H), 6.96 (d, *J* = 7.6 Hz, 1H), 6.91 – 6.87 (m, 2H), 6.82 (dd, *J* = 8.2, 1.9 Hz, 1H), 6.63 (dd, *J* = 17.6, 10.8 Hz, 1H), 5.67 (dd, *J* = 17.6, 0.8 Hz, 1H), 5.10 (dd, *J* = 10.8, 0.8 Hz, 1H), 3.79 (t, *J* = 6.4 Hz, 2H), 3.70 (t, *J* = 6.4 Hz, 2H), 1.74 – 1.61 (m, 4H), 1.45 – 1.33 (m, 4H), 1.30 – 1.21 (m, 4H). ^{13}C NMR (126 MHz, $CDCl_3$) δ 159.36, 159.18, 151.75, 151.46, 147.72, 147.55, 138.98, 136.83, 132.43, 132.18, 132.04, 129.72, 129.45, 129.41, 128.53, 127.20, 126.14, 125.14, 123.40, 122.23, 118.75, 114.52, 114.01, 113.97, 112.19, 68.03, 67.91, 29.36, 29.34, 29.31, 26.08, 26.04.

MALDI-TOF: calcd for $C_{50}H_{45}N_3O_2S$:751.3, found: 751.3 [M^+], Anal: Calcd for $C_{50}H_{45}N_3O_2S$: C, 79.86; H, 6.03; N, 5.59; S, 4.26; found: C, 80.01; H, 5.98; N, 5.50; S, 4.32.

General polymerization procedure for polymers

The polymers were synthesized by free radical polymerization using azodiisobutyronitrile (AIBN) as radical initiator and THF as solvent. AIBN was recrystallized from diethyl ether and THF was freshly distilled to remove the stabilizer before use. To synthesize the polymers, the monomer and AIBN (2 mol% of the total amount of monomers) were dissolved in THF with total concentration of ~ 0.2 g mL^{-1}, which were then stirred at 50 ^{o}C for 48 hours under argon atmosphere. After cooling to room temperature, the mixture was precipitated into acetone and methanol subsequently. The mixture was filtered and dried under vacuum to give the desired polymers in yields of 63~74%.

BP02 Mon-Ac (0.948 mmol, 0.2948 g), Mon-TRZ (0.050 mmol, 0.0167 g), Mon-PhPe (0.002 mmol, 0.0011 g) were used in the polymerization to provide the polymer (0.22 g) in yield of 71%. ^{1}H NMR (500 MHz, $CDCl_3$) δ 8.62 (s, 1H), 7.52 – 7.26 (m, 8H), 7.23 – 7.10 (m, 6H), 6.99 – 6.22 (m, 50H), 5.90 (s, 14H), 2.20 (d, *J* = 69.3 Hz, 7H), 1.81 – 1.18 (m, 55H). ^{13}C NMR (126 MHz, $CDCl_3$) δ 140.62, 129.68, 126.36, 125.03, 120.45, 113.67, 53.42, 35.78, 31.13. M_n=23.7 k Da, PDI=1.63

BP05 Mon-Ac (0.945 mmol, 0.2939 g), Mon-TRZ (0.050 mmol, 0.0167 g), Mon-PhPe (0.005 mmol, 0.0027 g) were used in the polymerization to provide the polymer (0.21 g) in yield of 68%. ^{1}H NMR (500 MHz, $CDCl_3$) δ 8.62 (s, 1H), 7.28 (d, *J* = 45.6 Hz, 9H), 7.25 – 7.10 (m, 9H), 6.82 (d, *J* = 211.8 Hz, 57H), 5.90 (s, 15H), 2.20 (d, *J* = 65.7 Hz, 8H), 1.81 – 1.18 (m, 60H). ^{13}C NMR (126 MHz, $CDCl_3$) δ 140.62, 129.67, 126.28, 125.12, 120.44, 113.62, 53.42, 40.67, 35.78, 31.15. M_n=21.4 k Da, PDI=1.80

BP10 Mon-Ac (0.940 mmol, 0.2923 g), Mon-TRZ (0.050 mmol, 0.0167 g), Mon-PhPe (0.010 mmol, 0.0054 g) were used in the polymerization to provide the polymer (0.23 g) in yield of 74%. ^{1}H NMR (500 MHz, $CDCl_3$) δ 8.62 (s, 1H), 7.51 – 7.26 (m, 9H), 7.25 – 7.08 (m, 9H), 6.83 (d, *J* = 211.0 Hz, 51H), 5.90 (s, 14H), 2.65 – 1.90 (m, 7H), 1.90 – 1.17 (m, 59H). ^{13}C NMR (126 MHz, $CDCl_3$) δ 140.60, 140.59, 129.72, 129.67, 126.30, 126.26, 125.08, 125.05, 120.45, 113.65, 113.60, 77.26, 77.01, 76.76, 53.42, 35.79, 31.15, 0.00. M_n=24.3 k Da, PDI=1.60

Ctrl-BP05 Mon-Ac (0.995 mmol, 0.3094 g), Mon-PhPe (0.005 mmol, 0.0027 g) were used in the polymerization to provide the polymer as (0.22 g) in yield of 71%. ^{1}H NMR (500 MHz, $CDCl_3$) δ 7.56 (d *J* = 7.8 Hz, 1H), 7.46 – 7.42 (m, 2H), 7.42 – 7.26 (m, 21H), 7.24 – 7.14 (m, 12H), 7.10 – 6.19 (m, 135H), 6.18 – 5.70 (m, 35H), 2.53 – 1.96 (m, 17H), 1.91 – 1.12 (m, 147H). ^{13}C NMR (126 MHz, $CDCl_3$) δ 141.55, 140.58, 130.55, 129.69, 126.29, 125.08, 120.47, 113.64, 53.42, 35.80, 31.22. M_n=22.4 k Da, PDI=1.76

GP05 Mon-Ac (0.945 mmol, 0.2939 g), Mon-CF (0.050 mmol, 0.0236 g), Mon-TBPAD (0.005 mmol, 0.0045 g) were used in the polymerization to provide the polymer (0.22 g) in yield of 69%. ^{1}H NMR (500 MHz, $CDCl_3$) δ 8.64 (s, 1H), 8.18 (s, 1H), 7.62 (s, 1H), 7.08 – 6.21 (m, 88H), 5.91 (s, 22H), 2.62 – 1.93 (m, 13H), 1.52 (s, 90H), 1.26 (d, *J* = 4.3 Hz, 2H). ^{13}C NMR (126 MHz, $CDCl_3$) δ 140.66, 129.68, 129.19, 126.29, 125.04, 120.52, 113.60, 35.81, 31.14. M_n=28.1 k Da, PDI=1.95

GP10 Mon-Ac (0.940 mmol, 0.2923 g), Mon-CF (0.050 mmol, 0.0236 g), Mon-TBPAD (0.010 mmol, 0.0090 g) were used in the polymerization to provide the polymer (0.21 g) in yield of 66%. ^{1}H NMR (500 MHz, $CDCl_3$) δ 8.64 (s, 1H), 8.18 (s, 1H), 7.62 (s, 1H), 7.32 (m, 13H), 7.24 – 7.10 (m, 11H), 7.09 – 6.21 (m, 79H), 5.90 (s, 20H), 2.50 – 1.90 (m, 11H), 1.52 (s, 82H), 1.26 (d, *J* = 4.6 Hz, 4H). ^{13}C NMR (126 MHz, $CDCl_3$) δ 141.41, 140.60, 130.49, 129.74, 129.13, 126.31, 125.06, 120.44, 113.59, 35.78, 31.41, 31.16. M_n=24.7 k Da, PDI=1.87

GP15 Mon-Ac (0.935 mmol, 0.2908 g), Mon-CF (0.050 mmol, 0.0236 g), Mon-TBPAD (0.015 mmol, 0.0135 g) were used in the polymerization to provide the polymer (0.21 g) in yield of 63%. ^{1}H NMR (500 MHz, $CDCl_3$) δ 8.64 (s, 1H), 8.18 (s, 1H), 7.62 (s, 1H), 7.10 – 6.21 (m, 82H), 5.91 (s, 21H), 2.57 – 1.89 (m, 11H), 1.52 (s, 82H), 1.25 (s, 4H). ^{13}C NMR (126 MHz, $CDCl_3$) δ 140.64, 129.68, 129.23, 126.25, 125.04, 120.53, 113.65, 35.82, 31.19. M_n=25.4 k Da, PDI=1.84

Ctrl-GP10 Mon-Ac (0.990 mmol, 0.3079 g), Mon-TBPAD (0.010 mmol, 0.0090 g) were used in the polymerization to provide the polymer (0.21 g) in yield of 68%. ^{1}H NMR (500 MHz, $CDCl_3$) δ 7.17 (m, 7H), 7.09 – 6.20 (m, 19H), 5.91 (s, 5H), 2.20 (m, 63.5 Hz, 3H), 1.41 (m, 19H), 1.26 (s, 1H). ^{13}C NMR (126 MHz, $CDCl_3$) δ 140.68, 129.68, 126.25, 125.06, 120.52, 113.59, 35.81, 31.16. M_n=23.1 k Da, PDI=1.99.

RP05 Mon-Ac (0.945 mmol, 0.2939 g), Mon-CN (0.050 mmol, 0.0192 g), Mon-NTTPA (0.005 mmol, 0.0037 g) were used in the polymerization to provide the polymer (0.21 g) in yield of 65%. ^{1}H NMR (500 MHz, $CDCl_3$) δ 8.55 (s, 1H), 8.22 (s, 1H), 6.83 (d, J = 209.6 Hz, 59H), 5.91 (s, 15H), 2.67 – 1.95 (m, 8H), 1.95 – 1.19 (m, 61H). ^{13}C NMR (126 MHz, $CDCl_3$) δ 140.59, 129.70, 126.23, 124.98, 120.50, 113.56, 35.78, 31.21 . M_n=27.6 k Da, PDI=1.73

RP10 Mon-Ac (0.940 mmol, 0.2923 g), Mon-CN (0.050 mmol, 0.0192 g), Mon-NTTPA (0.010 mmol, 0.0075 g) were used in the polymerization to provide the polymer (0.22 g) in yield of 68%. ^{1}H NMR (500 MHz, $CDCl_3$) δ 8.56 (s, 1H), 8.28 (s, 1H), 6.83 (d, J = 208.3 Hz, 59H), 5.91 (s, 15H), 2.66 – 1.90 (m, 10H), 1.95 – 1.19 (m, 65H). ^{13}C NMR (126 MHz, $CDCl_3$) δ 140.61, 129.70, 126.27, 125.06, 120.49, 113.57, 35.82, 31.22. M_n=26.4 k Da, PDI=1.83

RP15 Mon-Ac (0.935 mmol, 0.2908 g), Mon-CN (0.050 mmol, 0.0192 g), Mon-NTTPA (0.015 mmol, 0.0113 g) were used in the polymerization to provide the polymer (0.23 g) in yield of 72%. ^{1}H NMR (500 MHz, $CDCl_3$) δ 8.74 – 8.48 (m, 1H), 8.27 (s, 1H), 8.04 (s, 1H), 7.71 – 7.50 (m, 2H), 7.50 – 7.11 (m, 24H), 7.07 – 6.23 (m, 61H), 6.20 – 5.49 (m, 16H), 3.92 (m, 1H), 2.74 – 1.88 (m, 9H), 1.88 – 0.54 (m, 72H). ^{13}C NMR (126 MHz, $CDCl_3$) δ 141.32, 140.63, 130.61, 129.64, 129.03, 128.21, 126.31, 124.99, 120.44, 114.02, 113.55, 40.79, 35.78, 31.34, 31.19. M_n=24.0 k Da, PDI=1.88

Ctrl-RP15 Mon-Ac (0.985 mmol, 0.3063 g), Mon-NTTPA (0.015 mmol, 0.0113 g) were used in the polymerization to provide the polymer (0.24 g) in yield of 74%. ^{1}H NMR (500 MHz, $CDCl_3$) δ 7.59 – 7.12 (m, 6H), 7.11 – 6.22 (m, 16H), 5.91 (s, 4H), 2.53 – 1.92 (m, 2H), 1.61 (d, *J* = 84.2 Hz, 17H), 1.27 – 0.70 (m, 1H). ^{13}C NMR (126 MHz, $CDCl_3$) δ 140.68, 129.73, 126.29, 125.08, 120.47, 113.56, 35.81, 31.25. M_n=23.3 k Da, PDI=1.76

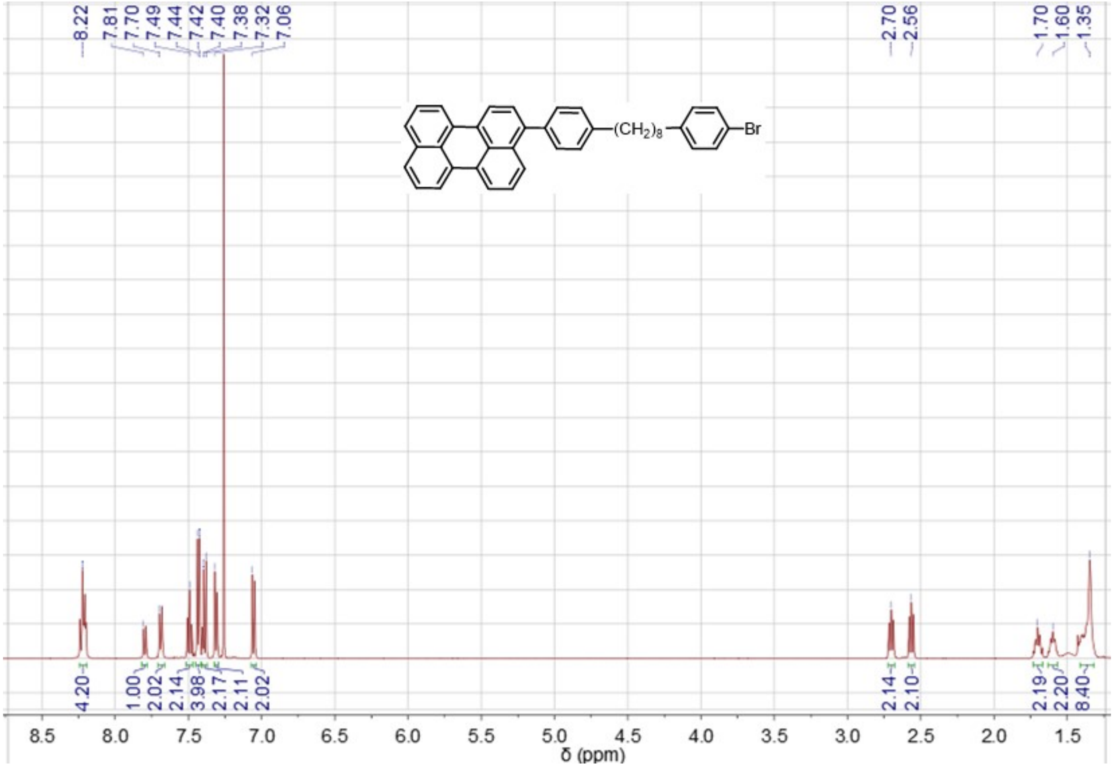

Figure S14. ^{1}H NMR spectrum of **3**.

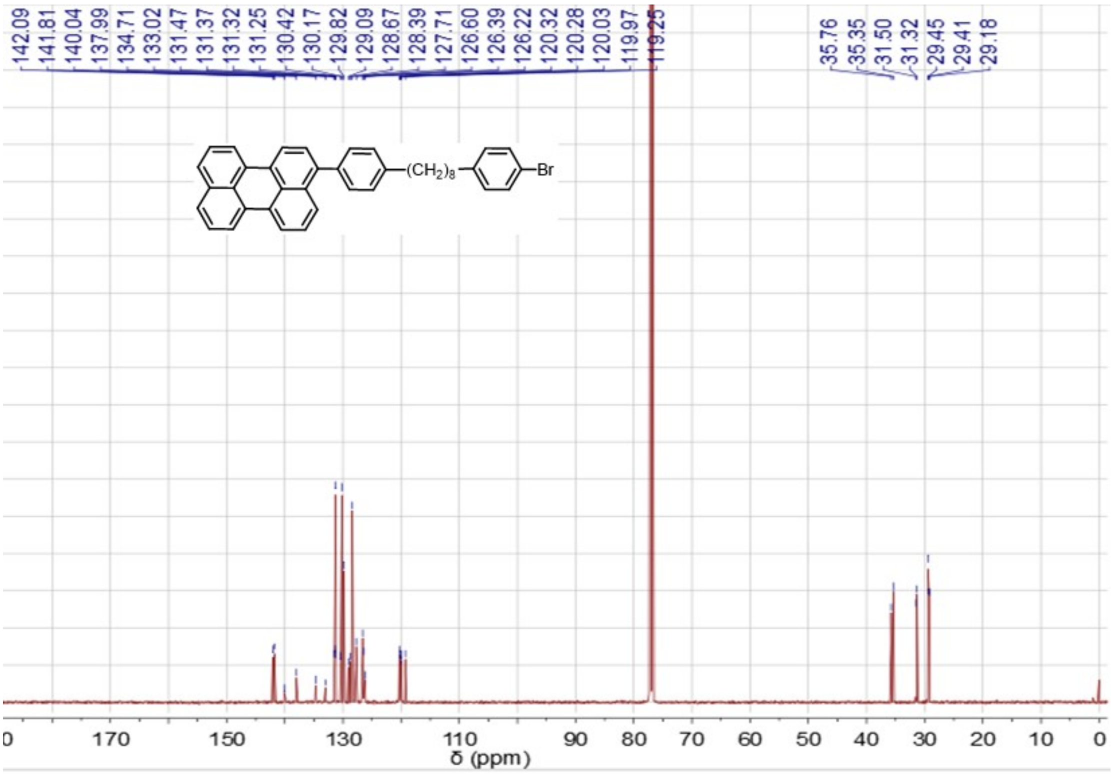

Figure S15. ^{13}C NMR spectrum of **3**.

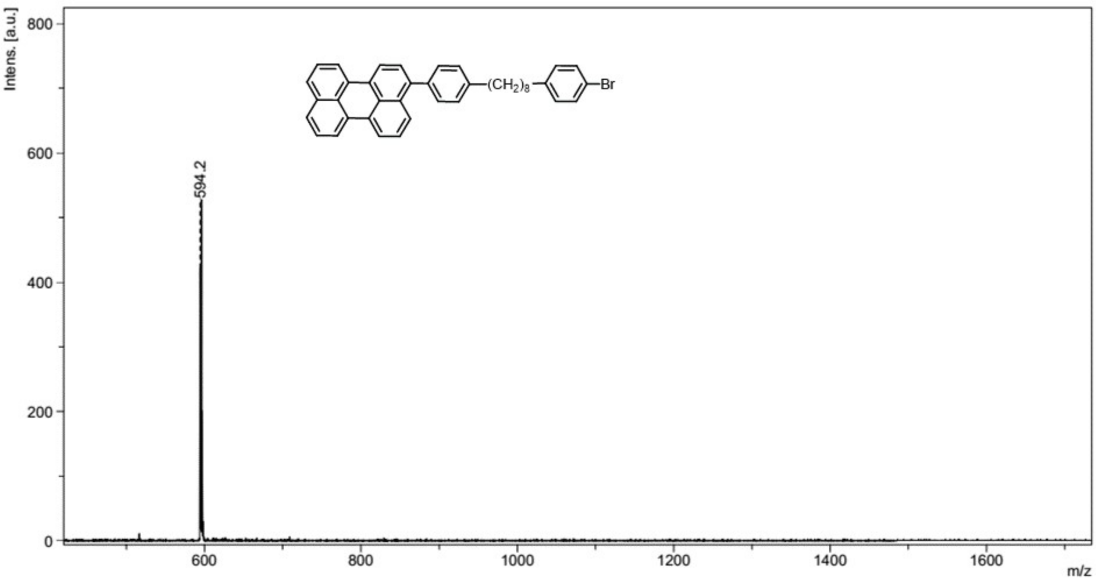

Figure S16. MALDI-TOF spectrum of **3**.

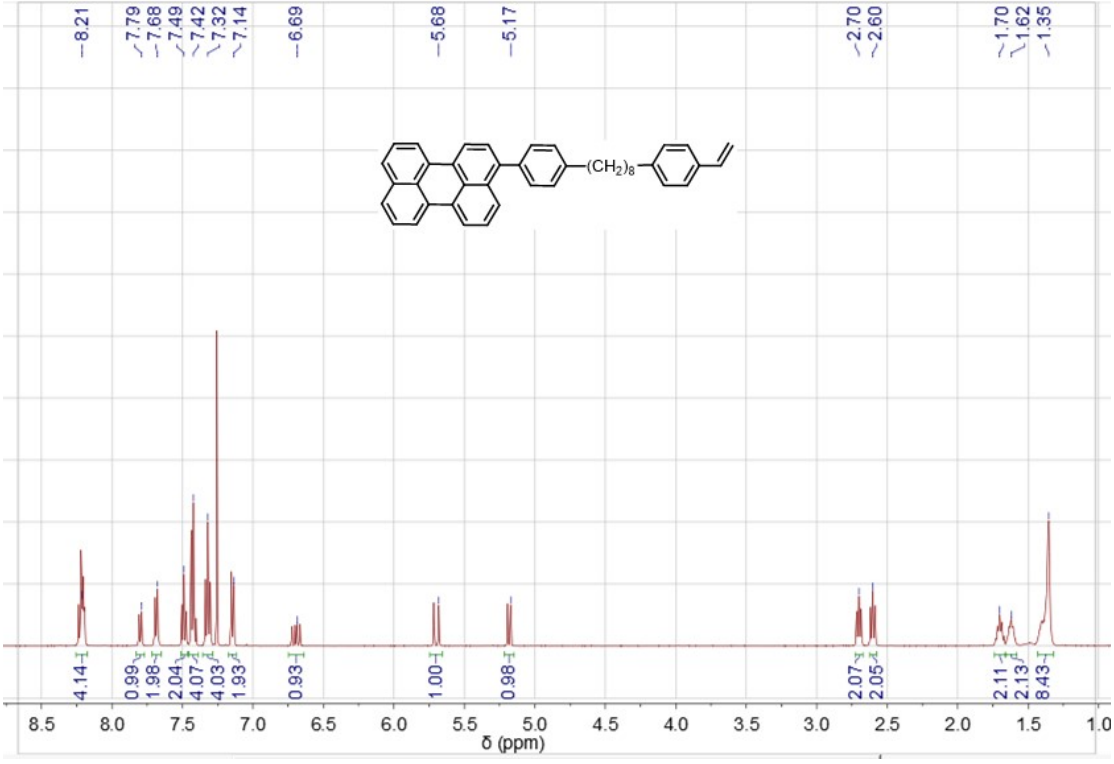

Figure S17. ^{1}H NMR spectrum of Mon-PhPe

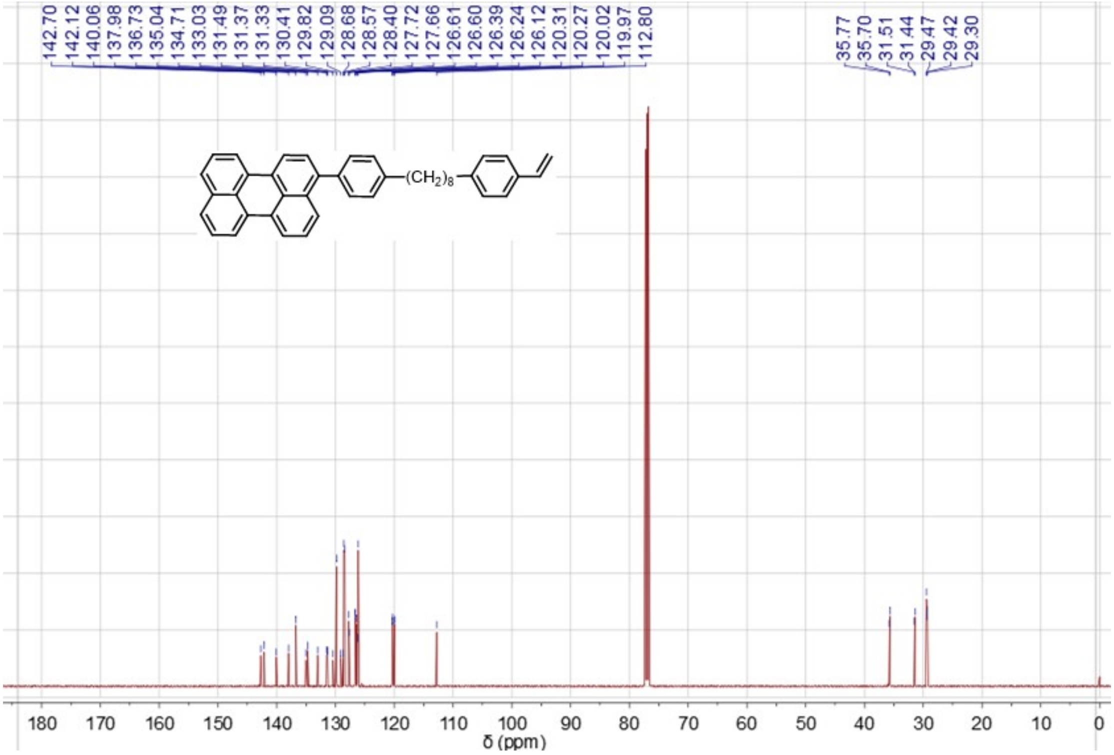

Figure S18. ^{13}C NMR spectrum of Mon-PhPe

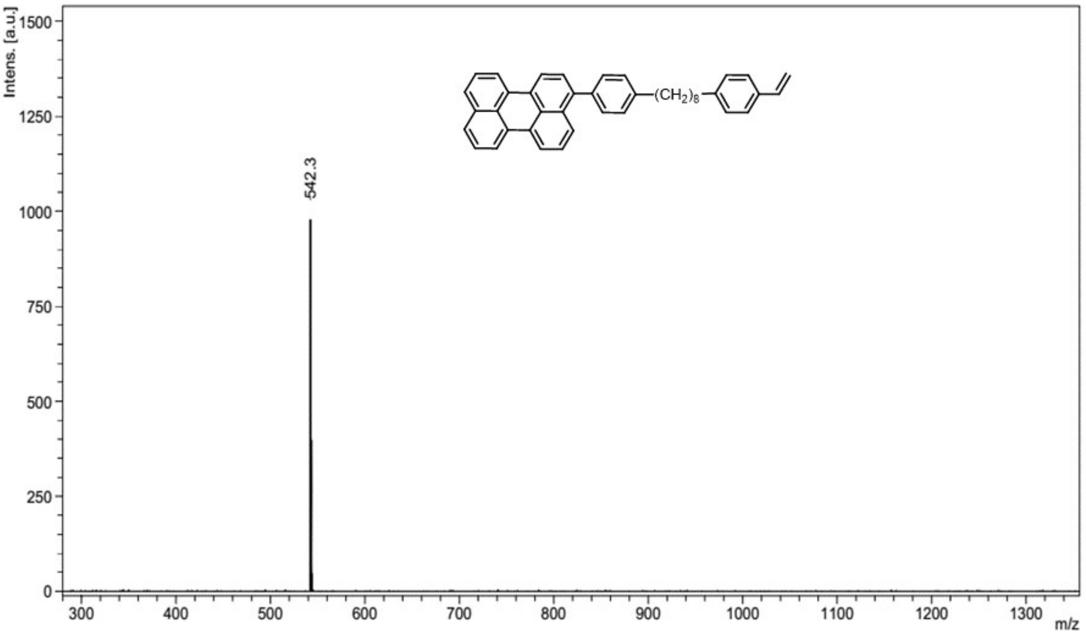

Figure S19. MALDI-TOF spectrum of Mon-PhPe

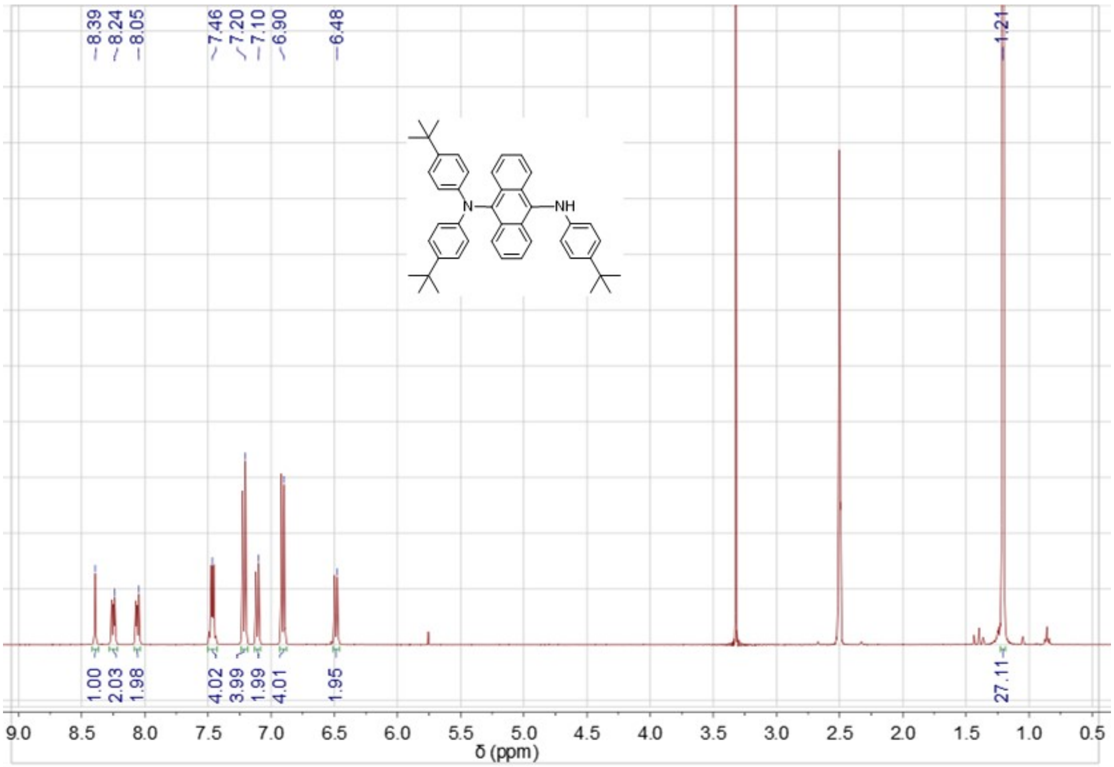

Figure S20. ^{1}H NMR spectrum of **5**.

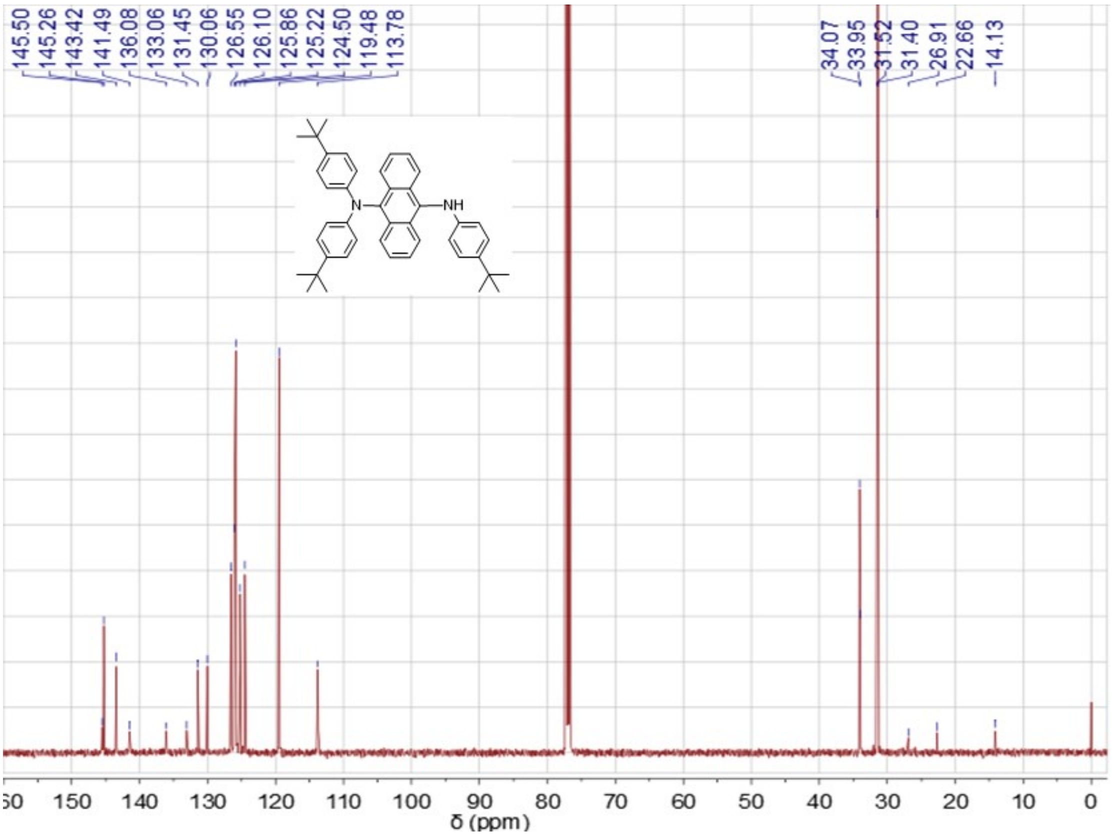

Figure S21. ^{13}C NMR spectrum of **5**.

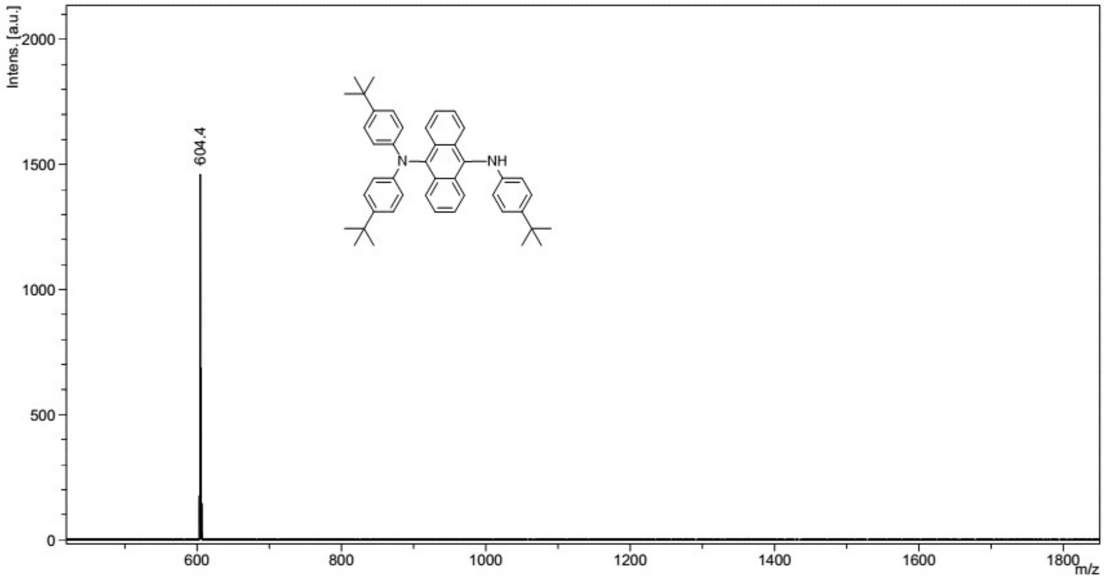

Figure S22. MALDI-TOF spectrum of **5**.

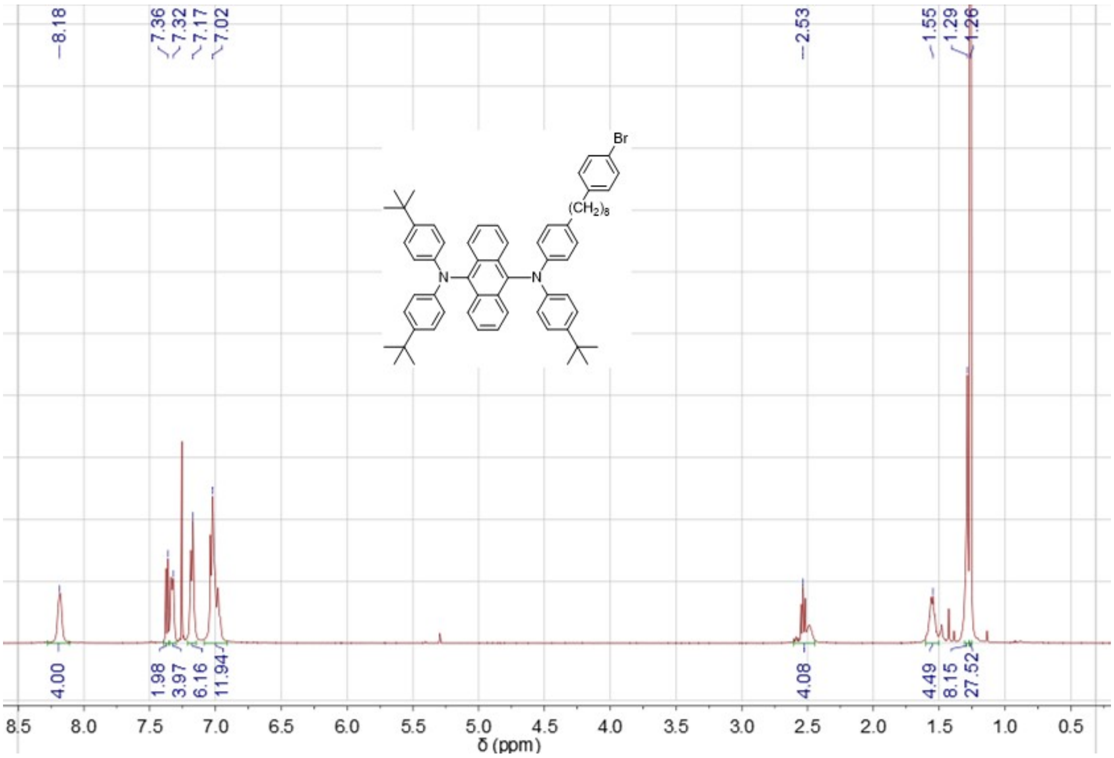

Figure S23. ^{1}H NMR spectrum of **6**.

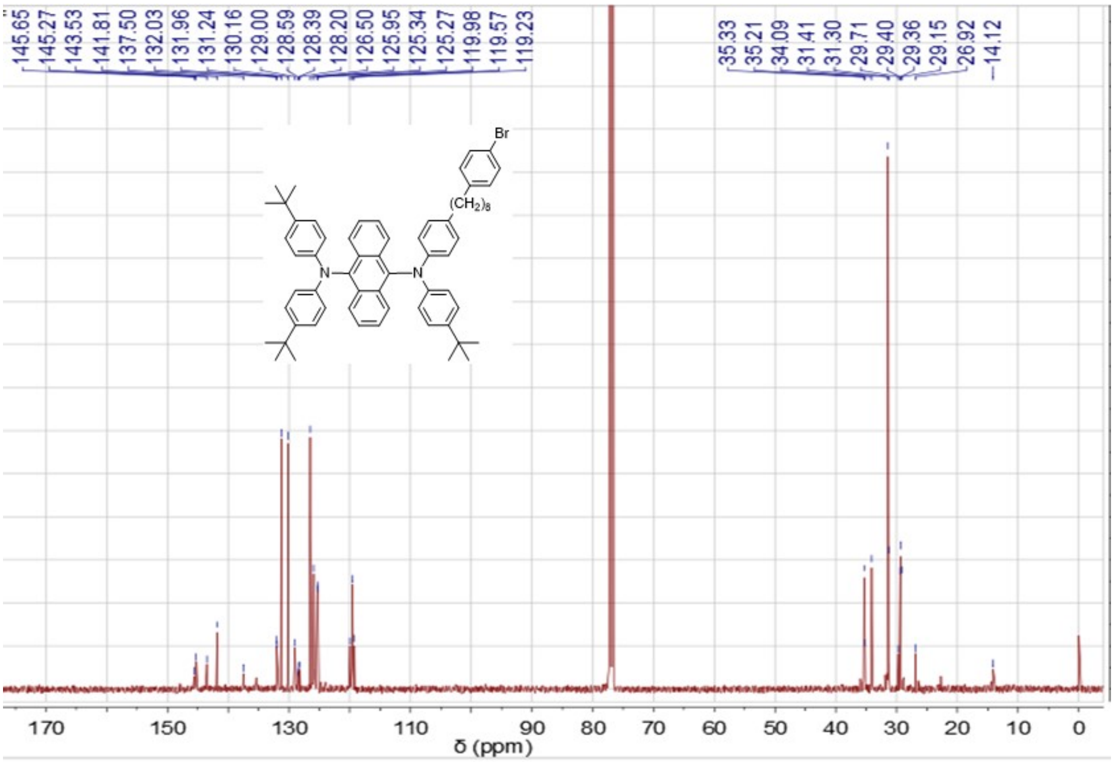

Figure S24. ^{13}C NMR spectrum of **6**.

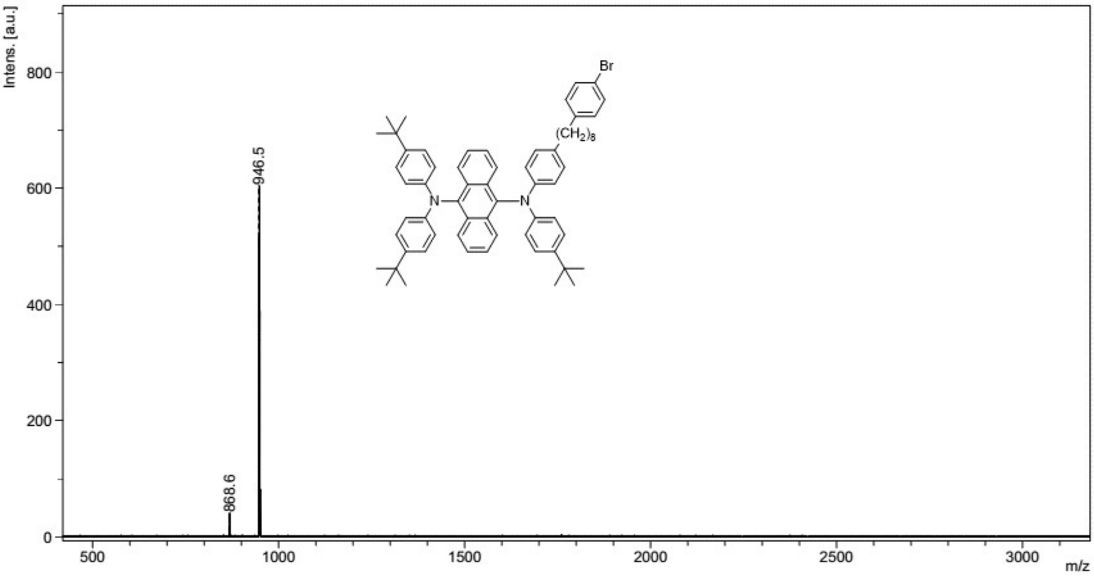

Figure S25. MALDI-TOF spectrum of **6**.

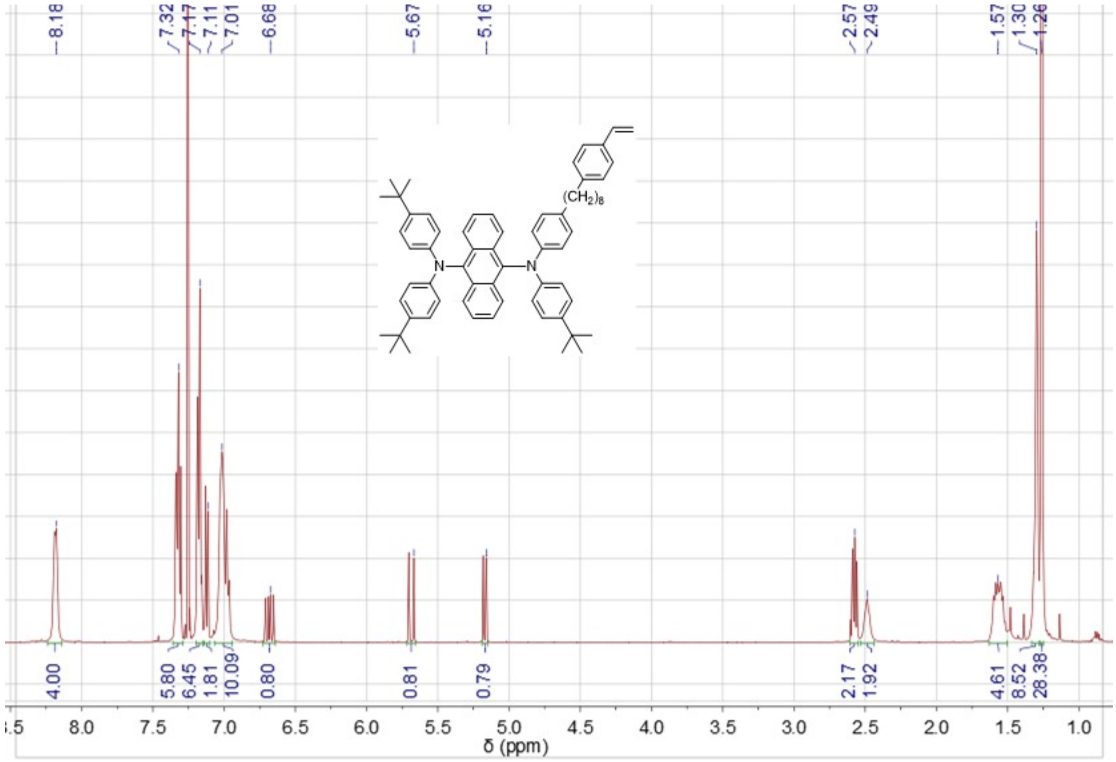

Figure S26. ^{1}H NMR spectrum of Mon-TBPAD.

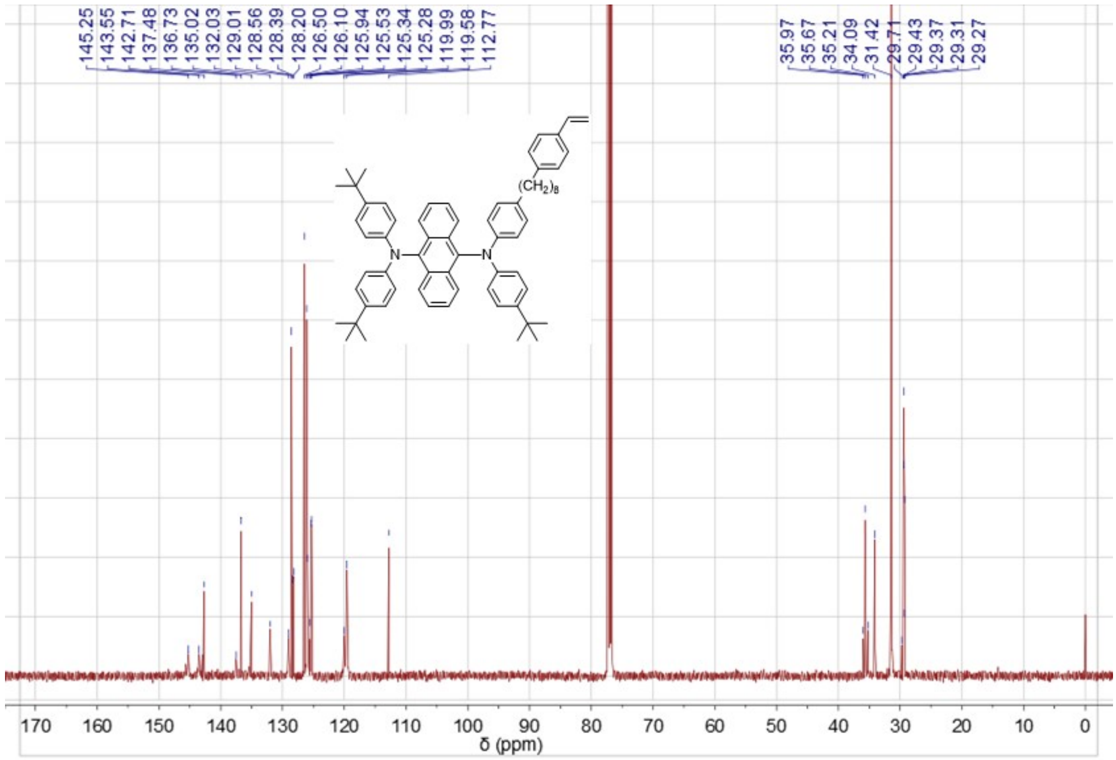

Figure S27. ^{13}C NMR spectrum of Mon-TBPAD.

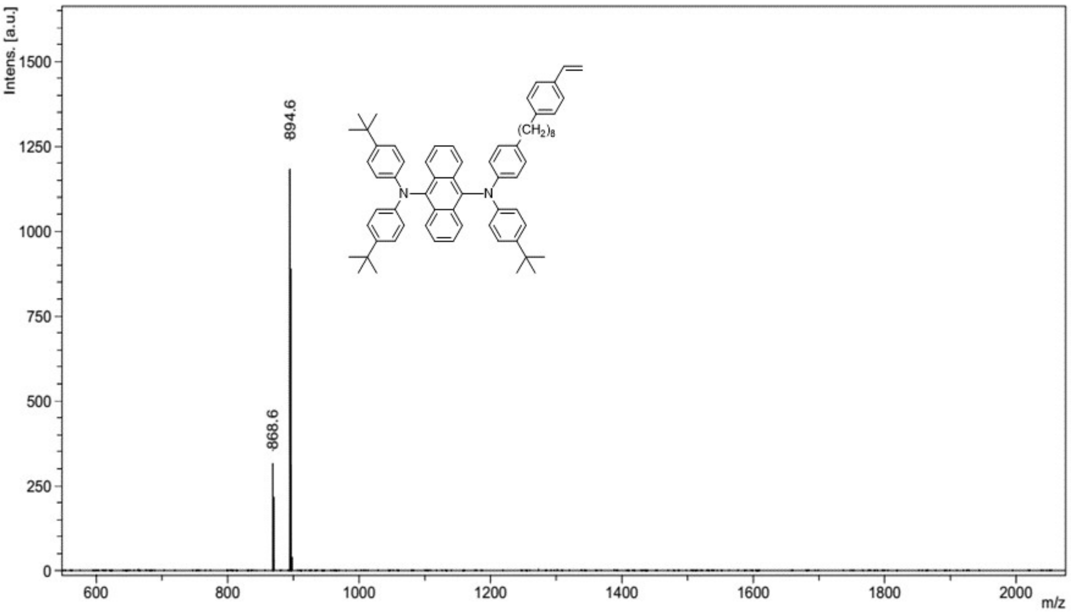

Figure S28. MALDI-TOF spectrum of Mon-TBPAD

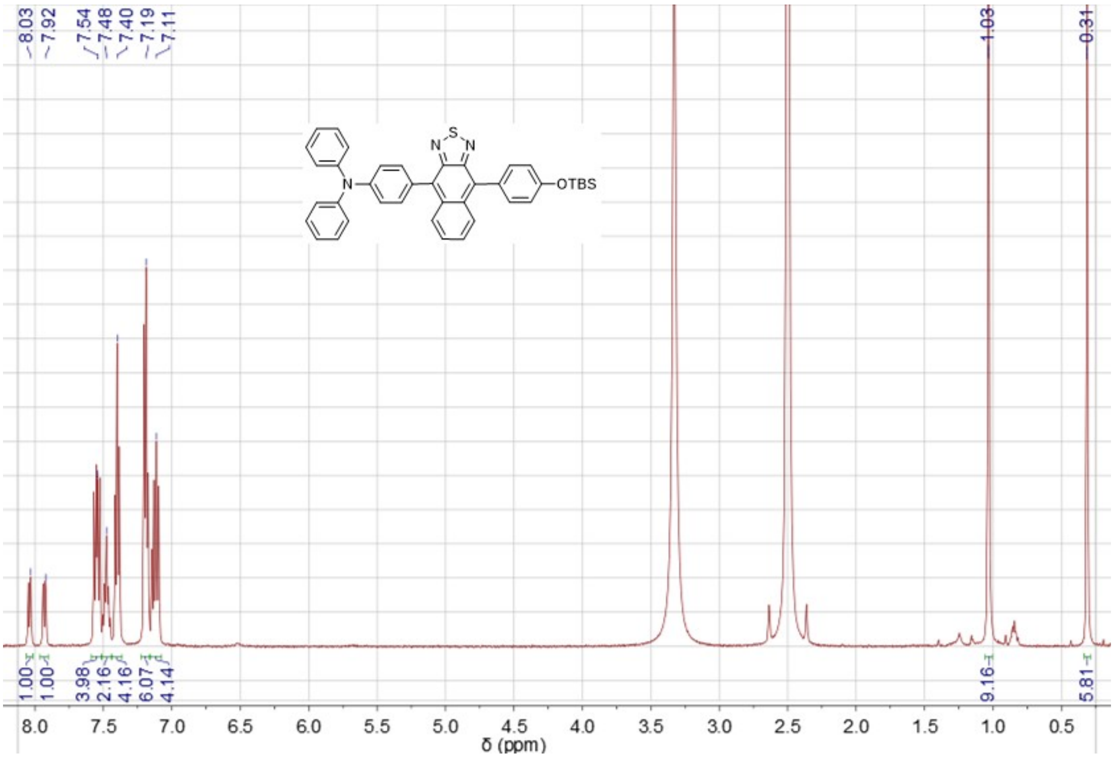

Figure S29. ^{1}H NMR spectrum of **8** with protecting group.

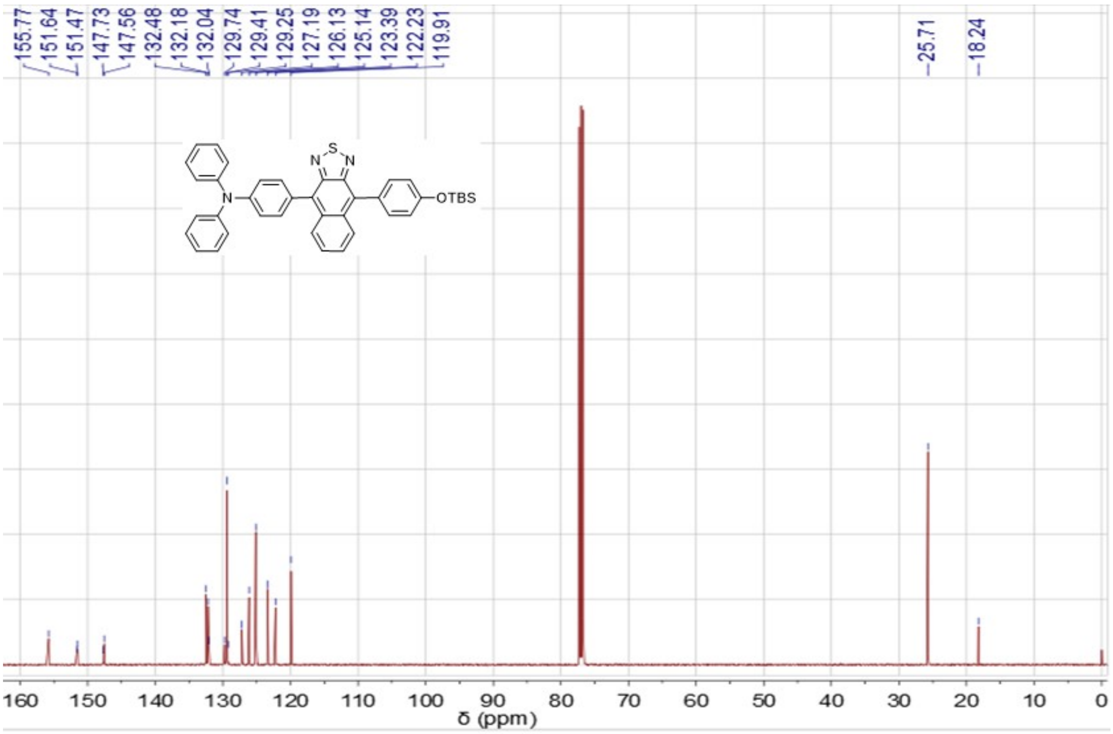

Figure S30. ^{13}C NMR spectrum of **8** with protecting group.

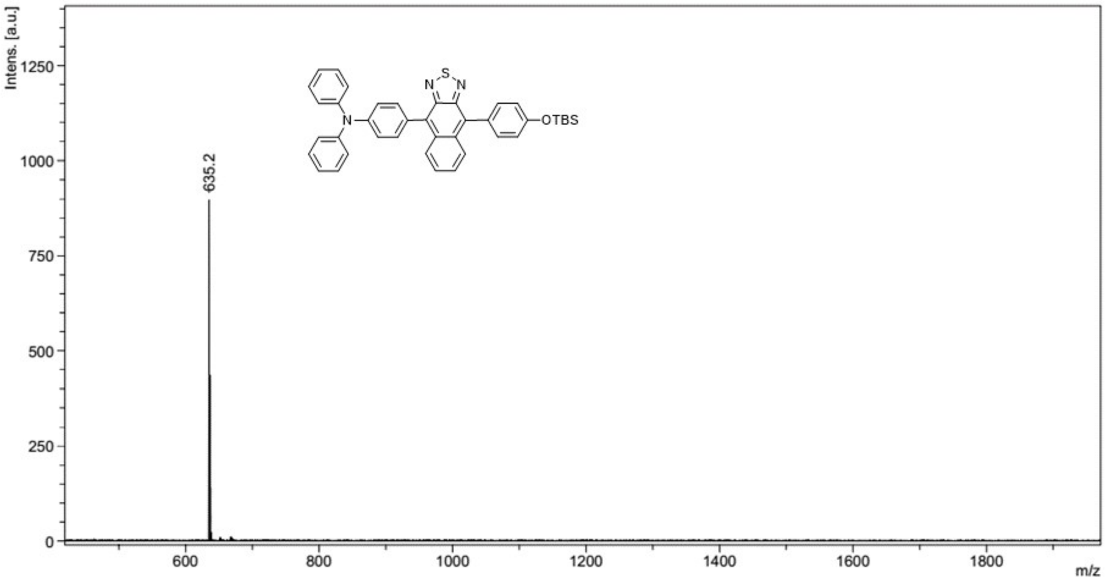

Figure S31. MALDI-TOF spectrum of **8** with protecting group.

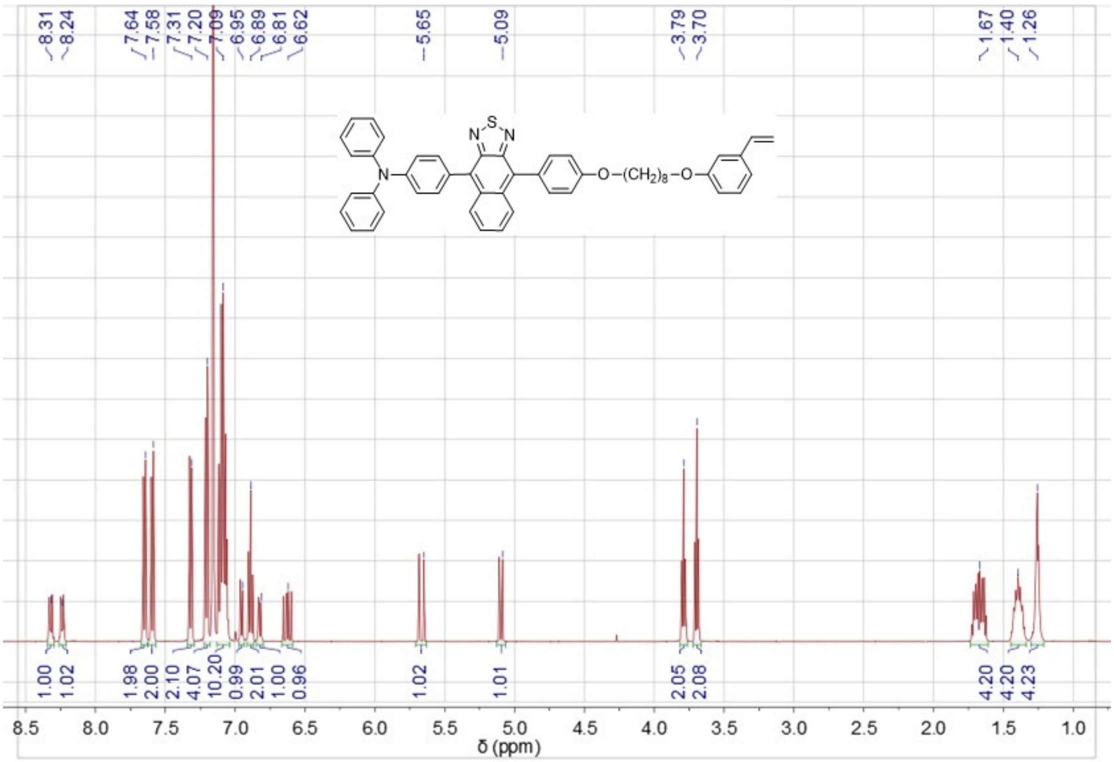

Figure S32. ^{1}H NMR spectrum of Mon-NTTPA

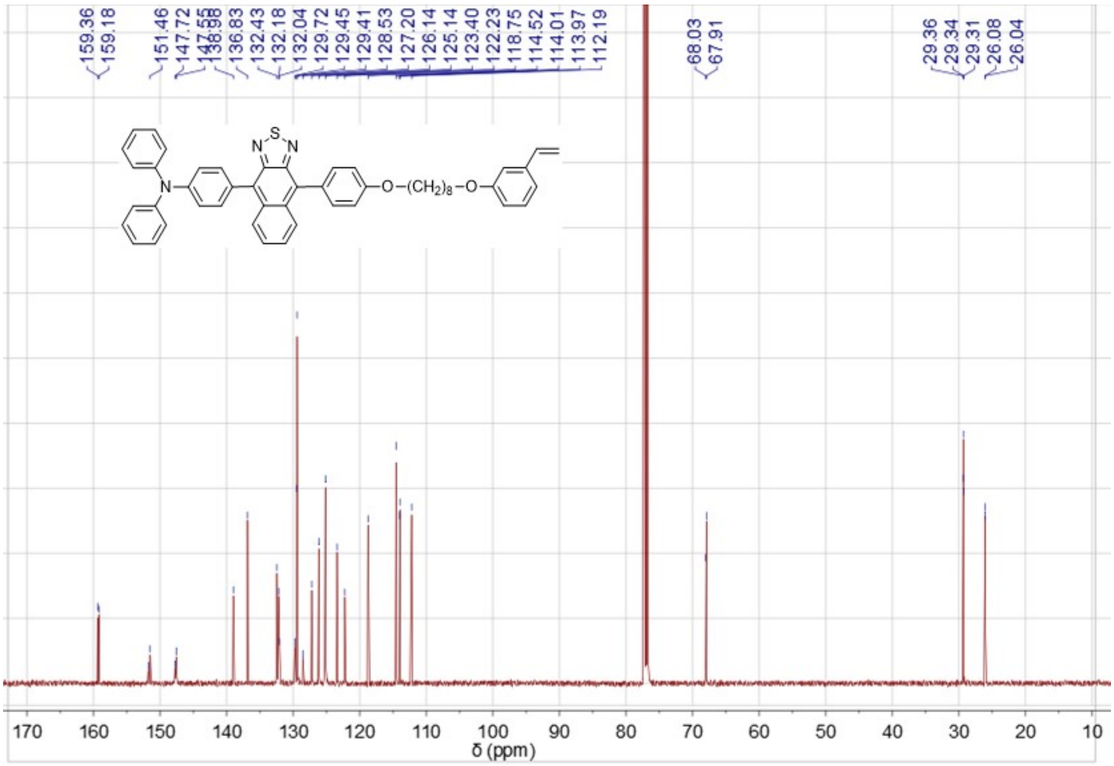

Figure S33. ^{13}C NMR spectrum of Mon-NTTPA

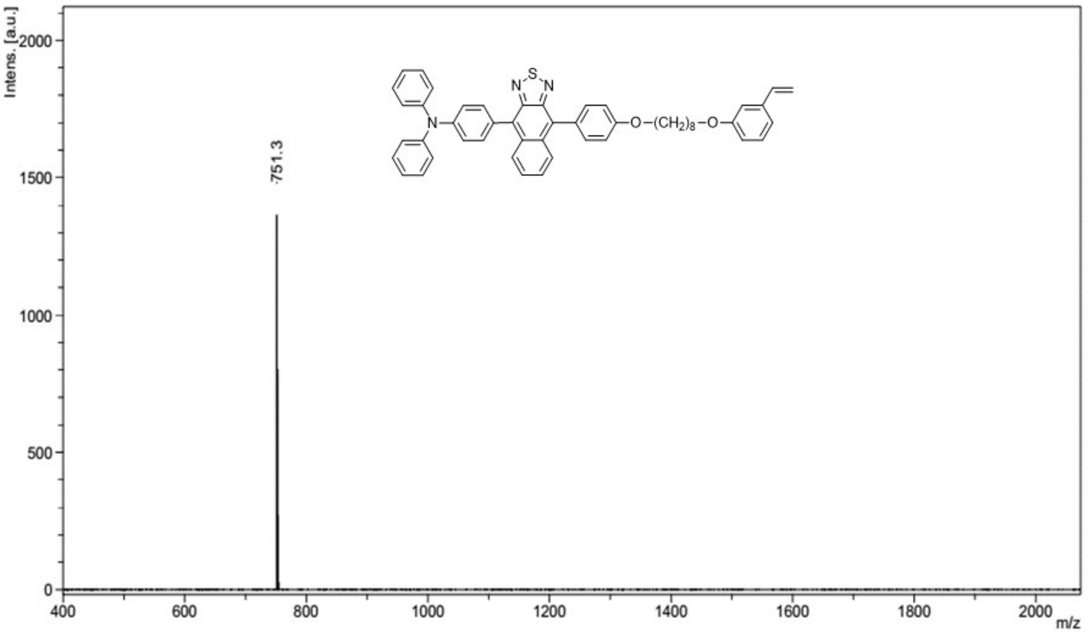

Figure S34. MALDI-TOF spectrum of Mon-NTTPA

References

[1] J. Hu, Q. Li, X. Wang, S. Shao, L. Wang, X. Jing, F. Wang, *Angew. Chem. Int. Ed*. **2019**, *58*, 8405.

[2] X. Cui, A. Charaf-Eddin, J. Wang, B. Le Guennic, J. Zhao, D. Jacquemin, *J. Org. Chem.* **2014**, *79*, 2038.

[3] D. Zhang, X. Song, M. Cai, L. Duan, *Adv. Mater*. 2018, 30, 1705250..

[4] L. Chen, H. Tong, Z. Xie, L. Wang, X. Jing, F. Wang, *J. Mater. Chem.*, **2011**, *21*, 15773

[5] Y. Avlasevich, K. Müllen, *J. Org. Chem.* **2007**, *72*, 10243

[6] S. Kantor, Ta-Cheng Sung, *Macromolecules.* **1992**, *25*, 2789.

[7] M. Uebe, D. Sakamaki, A, Ito, *ChemPlusChem*. **2019**, *84*, 1305 –1313.

[8] J. Hu, Q. Li, S. Shao, L. Wang, X. Jing, F. Wang, *Adv. Optical Mater.* **2020**, *8*,1902100.

[9] G. H. Xie, J. J. Luo, M. L. Huang, T. H. Chen, K. L. Wu, S. L. Gong, C. L. Yang, *Adv. Mater.* **2017**, *29*, 1604223.

[10] Y. Y. Hu, W. Q. Cai, L. Ying, D. J. Chen, X. Y. Yang, X. F. Jiang, S. J. Su, F. Huang, Y. Cao, *J. Mater. Chem. C* **2018**, *6*, 2690.

[11] X. Zeng, J. J. Luo, T. Zhou, T. H. Chen, X. Zhou, K. L. Wu, Y. Zou, G. H. Xie, S. L. Gong, C. L. Yang, *Macromolecules* **2018**, *51*, 1598.

[12] X. Zhou, M. L. Huang, X. Zeng, C. Zhong, G. H. Xie, X. S. Cao, C. G. Yang, C. L. Yang, *Polym. Chem.* **2020**, *11*, 3481..

[13] X. Liu, J. Rao, X. Li, S. Wang, J. Ding, L. Wang, *iScience* **2019**, *15*, 147.

[14] C. Li, Z. Ren, X. Sun, H. Li, S. Yan, *Macromolecules* **2019**, *52*, 2296.

[15] S. Y. Lee, T. Yasuda, H. Komiyama, J. Lee, C. Adachi, *Adv. Mater*. **2016**, *28*, 4019.

[16] C. Li, Y. Wang, D. Sun, H. Li, X. Sun, D. Ma, Z. Ren, S. Yan, *ACS Appl. Mater. Interfaces.* **2018**, *10*, 5731

[17] H. J. Kim, C. Lee, M. Godumala, S. Choi, S. Y. Park, M. J. Cho, S. Park, D. H. Choi, *Polym. Chem.* **2018**, *9*, 1318.

[18] J. Rao, L. Yang, X. Li, L. Zhao, S. Wang, J. Ding, L. Wang, *Angew. Chem. Int. Ed.* **2020**, *60*, 9535.

[19] J. Rao, L. Yang, X.Li, L. Zhao, S. Wang, H. Tian, J. Ding, L. Wang, *Angew. Chem. Int. Ed.* **2021**. 59, 17903.

[20] X. Zhou, M. Huang, X. Zeng, T. Chen, G. Xie, X. Yin, C. Yang, *Polym. Chem.* 2019, 10, 4201.

[21] Y. Liu, L. Hua, S. Yan, Z. Ren, *Nano Energy* **2020**, *73*, 104800.

[22] T. Wang, K. Li, B. Yao, Y. Chen, H. Zhan, Z. Xie, G. Xie, X. Yi, Y. Cheng, *Adv. Funct. Mater.* **2020**, *30*, 2002493.

[23] T. Wang, B. Yao, K. Li, Y. Chen, H. Zhan, X. Yi, Z. Xie, Y. Cheng, *Adv. Optical Mater.* **2021**, 9, 2001981.